ERDC/GSL TR-15-32

Geotechnical and Structures Laboratory

US Army Corps
of Engineers®
Engineer Research and
Development Center

ERDC
INNOVATIVE SOLUTIONS
for a safer, better world

Airfield Damage Repair Modernization Program

AM2 Modified 2-1 Lay Pattern Evaluation under F-15E Traffic

Lyan Garcia, Julie Heiser, Timothy W. Rushing,
Chase T. Bradley, Jeb S. Tingle, and Craig A. Rutland

August 2015

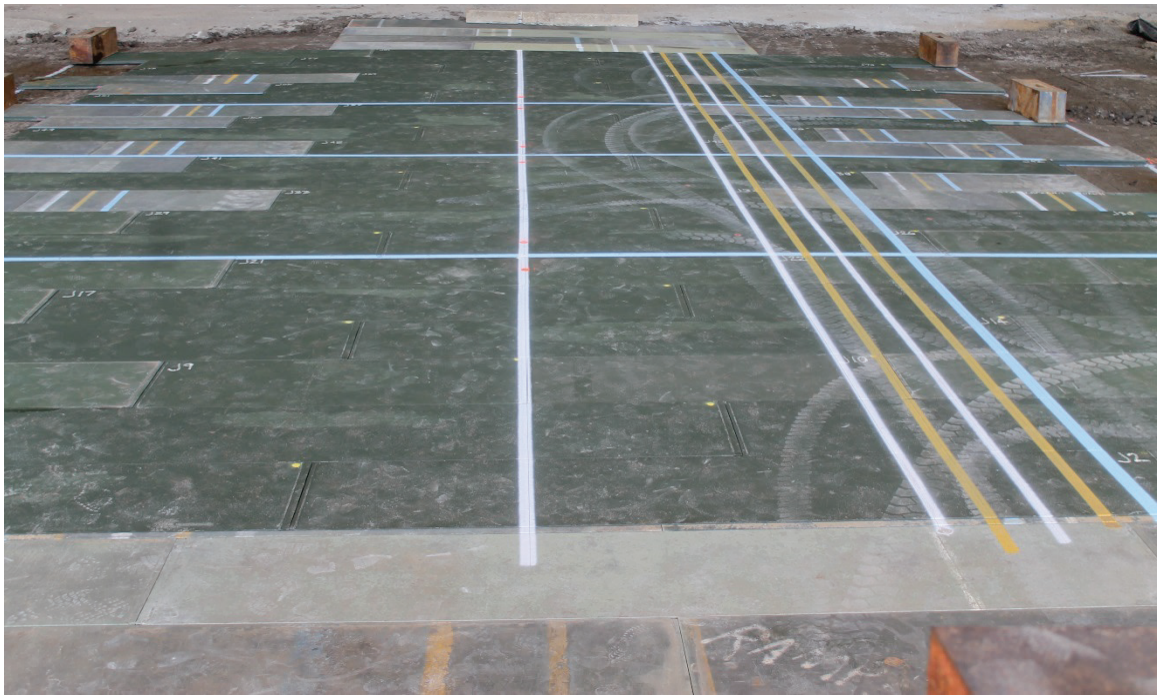

The U.S. Army Engineer Research and Development Center (ERDC) solves the nation's toughest engineering and environmental challenges. ERDC develops innovative solutions in civil and military engineering, geospatial sciences, water resources, and environmental sciences for the Army, the Department of Defense, civilian agencies, and our nation's public good. Find out more at www.erdc.usace.army.mil.

To search for other technical reports published by ERDC, visit the ERDC online library at http://acwc.sdp.sirsi.net/client/default.

ERDC/GSL TR-15-32
August 2015

AM2 Modified 2-1 Lay Pattern Evaluation under F-15E Traffic

Lyan Garcia, Timothy W. Rushing, Chase T. Bradley, and Jeb S. Tingle

Geotechnical and Structures Laboratory
U.S. Army Engineer Research and Development Center
3909 Halls Ferry Road
Vicksburg, MS 39180-6199

Julie Heiser

Applied Research Associates
430 West 5th Street, Suite 700
Panama City, FL 32401

Craig A. Rutland, PhD

Engineering Division
Civil Engineering Branch
Air Force Civil Engineer Center
139 Barnes Drive, Suite 1
Tyndall AFB, FL 32403

Final report

Prepared for Headquarters, Air Force Civil Engineer Center
Tyndall Air Force Base, FL 32403-5319

Abstract

The U.S. Army Engineer Research and Development Center executed a program for the Air Force Civil Engineer Center and the Naval Air Systems Command (NAVAIR) that involved a series of full-scale tests of the AM2 airfield mat system in an effort to validate a model which predicts the performance of AM2 under different operational conditions. A key component of the test program was evaluating the AM2 installation patterns approved by NAVAIR, which included the 2-1 lay pattern that is used on runways and high-speed taxiways. Initial analyses of the results showed that the performance of the AM2 mat system installed in the 2-1 lay pattern decreased when compared to the standard brickwork pattern, largely because of sections resulting with two longitudinal joints. An alternative pattern was sought to improve the load-carrying capabilities of the system, and the results are provided in this report. The discussions herein summarize traffic tests that were conducted on what was called the "modified" 2-1 lay pattern, which amended the 2-1 lay pattern to eliminate the key contributor that reduced system performance (i.e., two continuous joints). The results showed a significant increase in passes-to-failure in comparison to the 2-1 lay pattern and the brickwork pattern.

Contents

Figures and Tables

Figures

Tables

Preface

This study was conducted for the U.S. Naval Air Systems Command (NAVAIR) Expeditionary Airfield (EAF) team and the U.S. Air Force Civil Engineer Center (AFCEC). Technical oversight was provided by Jeb S. Tingle.

The work was performed by the Airfields and Pavements Branch (APB) of the Engineering Systems and Materials Division (ESMD), U.S. Army Engineer Research and Development Center, Geotechnical and Structures Laboratory (ERDC-GSL). At the time of publication, Dr. John Rushing was Acting Chief, APB; Dr. Larry N. Lynch was Chief, ESMD; and Nicholas Boone was the Technical Director for Force Projection and Maneuver Support. The Acting Deputy Director of ERDC-GSL was Dr. Will McMahon, and the Acting Director was Dr. William P. Grogan.

LTC John T. Tucker III was the Acting Commander of ERDC, and Dr. Jeffery P. Holland was the Director.

Unit Conversion Factors

Multiply	By	To Obtain
cubic feet	0.02831685	cubic meters
feet	0.3048	meters
inches	0.0254	meters
kip-inches	112.948	newton-meters
pounds (force)	4.448222	newtons
pounds (force) per square foot	47.88026	pascals
pounds (force) per square inch	6.894757	kilopascals
pounds (mass)	0.45359237	kilograms
square feet	0.09290304	square meters
square inches	6.4516 E-04	square meters

1 Introduction

1.1 Background

1.1.1 Naval Air Systems Command Dynamic Interface Model

AM2 aluminum matting has been the primary temporary airfield matting system used by the U.S. military since the late 1960s. AM2 was developed by the U.S. Navy but has been adopted for use by the U.S. Air Force (USAF) and the U.S. Army for fixed-wing and rotary-wing operational surfaces. Over the years, AM2 has been modified to address limiting structural concerns. The current production version of AM2 is modification (Mod) 5.

An AM2 surface is comprised of interlocking 2-ft by 12-ft full panels and 2-ft by 6-ft half panels that are 1.5 in. thick. An AM2 mat expanse can be assembled to form runways, vertical takeoff and landing pads, taxiways, and aircraft parking areas. In 2012, the Naval Air Systems Command (NAVAIR) Expeditionary Airfield Team (EAF) partnered with the Air Force Civil Engineer Center (AFCEC) to sponsor a series of full-scale AM2 evaluations in an effort to validate a Dynamic Interface Model (DIM) developed by NAVAIR. The model was validated through laboratory subscale tests, but additional development and validation were required to accurately model the matting-soil interaction for various installation patterns. The U.S. Army Engineer Research and Development Center (ERDC) was tasked with these evaluations (Table 1). Individual AM2 configuration lay patterns were tested under simulated traffic with appropriate instrumentation at the connections to collect strain data for the DIM. Each test was compared to baseline performance data from full-scale testing conducted at the ERDC from 2005 through 2011 (Table 2).

1.1.2 AM2 certified configuration lay patterns

Descriptions of the placement, or lay, patterns shown in Table 1 (brickwork, 2-1, 3-4) are provided in *Expeditionary airfield AM2 mat certification requirements* (NAWCADLKE-MISC-48J200-0011). The individual patterns were established as part of an initiative to optimize the use of 6-ft half panels. The original AM2 shipping package, F44, contained sixteen 12-ft panels and four 6-ft panels. Each package was designed to allow assembly of two 108-ft-wide rows or four 54-ft-wide rows in a brickwork configuration

with no continuous longitudinal joints. The brickwork pattern assures excellent load-carrying capability of the system. Since 6-ft panels are used only for the row ends, more 12-ft panels are required for assembly. However, ship transportation of the mats across the globe led to a need for the mats to be shipped on an International Organization for Standardization (ISO) flat rack for compatibility with other containerized goods. A decision was made by the U.S. Navy to repackage AM2 into new shipping packages, which resulted in the development of the F71 and F72 shipping configurations.

Table 1. AM2 testing program.

Test sequence	Test name	AM2 lay pattern	Condition of AM2 mats	F-15E traffic	C-17 traffic
1	In-plane bow on asphalt surface	Brickwork	New	N/A	N/A
2	Vehicle braking test on asphalt surface	Brickwork	New	N/A	N/A
3	Brickwork on voided subgrade (CBR of 6)	Brickwork	New and refurbished	Yes	No
4	Brickwork on CBR of 6	Brickwork	New and refurbished	Yes	Yes
5	In-plane bow on CBR of 6	Brickwork	New	N/A	N/A
6	Opposite lay on CBR of 6*	Brickwork	New	Yes	Yes
7	3-4 lay on CBR of 6	3-4	New	Yes	Yes
8	2-1 lay on CBR of 6	2-1	New	Yes	Yes
9	Brickwork on voided subgrade (CBR of 6)	Brickwork	New	Yes	No
10	Brickwork on CBR of 6	Brickwork	New	Yes	Yes

*traffic applied parallel to long dimension of AM2 panels

Table 2. Summary of AM2 brickwork pattern subgrade sensitivity testing results.

Sustained Traffic Passes			
Subgrade Strength (CBR)	F-15E	C-17	Reference
6	1,500	1,500	Rushing and Tingle (2007)
10	3,000	6,000	Rushing et al. (2008)
15	4,100	7,000	Rushing and Mason (2008)
25	6,300	10,000*	Garcia et al. (2014a)
100	23,000	-	Garcia et al. (2014b)

* Failure was not achieved. Trafficking was stopped because of time constraints.

The F71 contains eighteen 12-ft mats, and the F72 contains eighteen 6-ft mats. The new configurations allow one F71 and one F72 to be placed end-to-end on a 20-ft ISO flat rack to optimize the use of the available space. The new package configuration also reduced confusion when designing a mat surface. In some instances, F44 packages were re-bundled with different numbers of 6-ft panels inside the 12-ft mat packages. Separating the panels into the F71 and F72 packages eliminated the need to include mixed sizes in packages and improved the accuracy of panel inventories.

The optimization of packaging and shipping of AM2 required equal numbers of 12-ft and 6-ft mat panels to be delivered with each AM2 order. Since only a fraction of the available 6-ft panels are needed to assemble a brickwork pattern, many 6-ft panels were unused. To optimize mat use, NAVAIR EAF created an allowance for two alternate lay patterns, the 2-1 and the 3-4 lay patterns.

The 2-1 lay pattern was designed for use on all aircraft operating surfaces, including runways and high-speed taxiways. The pattern consists of installing AM2 in a brickwork configuration for two rows. The third row is started with a single 12-ft panel and is then filled entirely with 6-ft panels to complete the desired width. The 2-1 lay pattern results in sections with two continuous 2-ft end (longitudinal) joints (Figure 1). The 3-4 lay pattern was designed only for parking or slow-speed secondary taxi areas and is not allowed for use on runways or high-speed primary taxiways. The 3-4 pattern consists of installing three rows of a brickwork pattern and then four rows of any matting that is available. Under worst-case conditions, the 3-4 pattern can result in as many as six continuous 2-ft end (longitudinal) joints.

Although the two patterns were approved by NAVAIR EAF, they had not been evaluated under simulated aircraft loading conditions to determine whether any reduction in the number of allowable passes was caused by the allowance of continuous longitudinal joints. Therefore, they were included in the test program. Results for the 3-4 lay pattern are reported in ERDC/GSL TR-14-38 (Rushing et al. 2014).

1.1.3 AM2 modified 2-1 configuration lay pattern

The report for the 2-1 lay pattern results is currently in development, but initial analyses showed that a reduction in performance in terms of sustainable aircraft passes of at least 30 percent occurred when compared

to the brickwork pattern for an AM2 surface placed on a California bearing ratio (CBR) of 6. This was largely attributed to the sections that consisted of two continuous end joints (Figure 1), where premature, consecutive rail failures occurred due to reduced support on each 2-ft end. The brickwork pattern, in comparison, provides better load transfer and improved end connector performance because it has an unsupported length of only one panel.

Figure 1. AM2 2-1 lay configuration pattern.

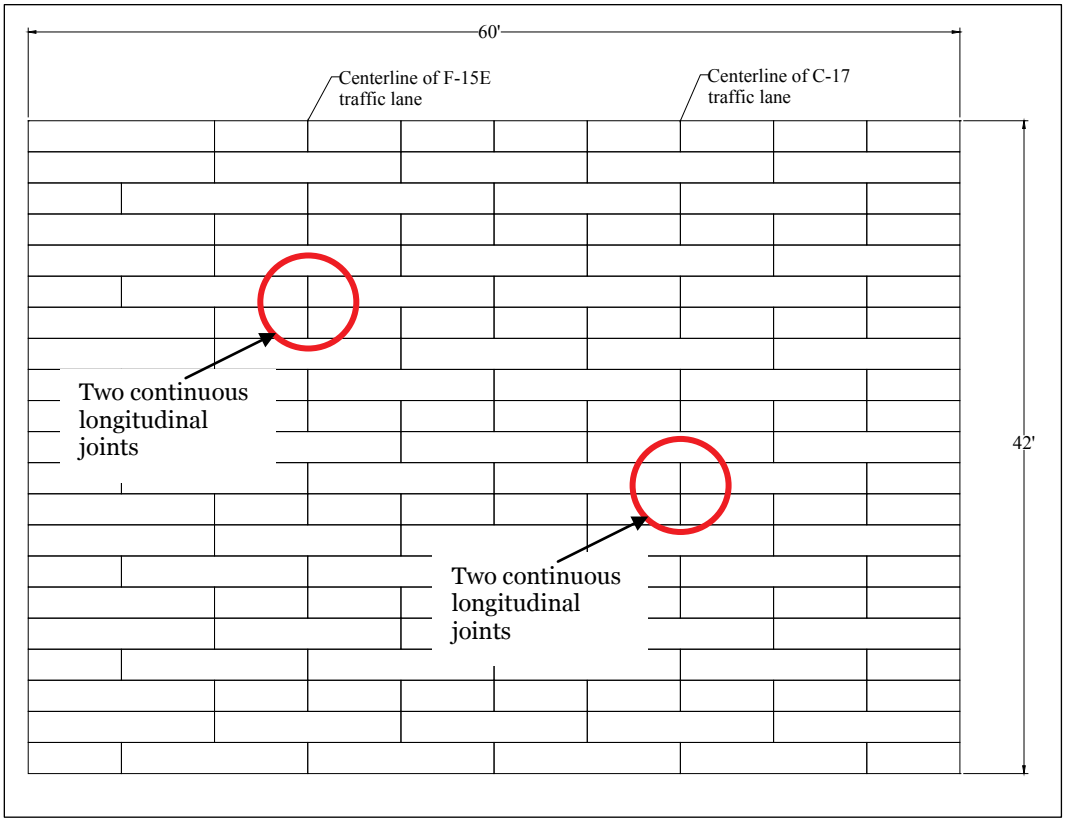

NAVAIR requires that a minimum CBR of 25 be used for construction of AM2 airfields that will allow C-17 aircraft operations, but it typically use this criterion for construction of all aircraft operating surfaces to reduce maintenance and repair activities. However, a minimum CBR of 4 is allowed for most other operations (NAWCADLKE-MISC-48J200-0011). Thus, there was concern as to the structural capabilities of the 2-1 lay pattern when installed on soft subgrades, mostly because it is approved for construction of runways and high-speed taxiways.

After completion of the 2-1 lay pattern test, AFCEC decided to investigate alternatives that could help improve the load-carrying capacity of the 2-1

lay pattern. One idea that arose was offsetting a joint 3 ft from the centerline on every other row to avoid sections with two continuous 2-ft ends. The result would be a staggered pattern that would ultimately be shifted 3 ft on each side of the test surface at several rows. Thus, AFCEC sponsored the evaluation of the configuration called the "modified" 2-1 lay pattern discussed in this report.

1.1.4 AM2 end connector critical stress location

After completion of the test program listed in Table 1, a thorough investigation of both the subgrade and the mat revealed that the manufacturer's drawing of the extrusion die for the AM2 end connector inadvertently omitted filleted corners in the locking bar channel, at the interface with the smallest cross-sectional area of the rail (Figure 2). Several modeling efforts showed these corners were areas of high stress concentration that eventually caused cracking along the upper underlap or lower overlap rails, which was damage commonly reported by Rushing and Tingle (2007), Rushing and Torres (2007), Rushing et al. (2008), Rushing and Mason (2008), and Garcia and Rushing (2013). An example of crack initiation at one of the corners is shown in Figure 3.

Figure 2. Corners with fillet omitted, as indicated by the dotted circles.

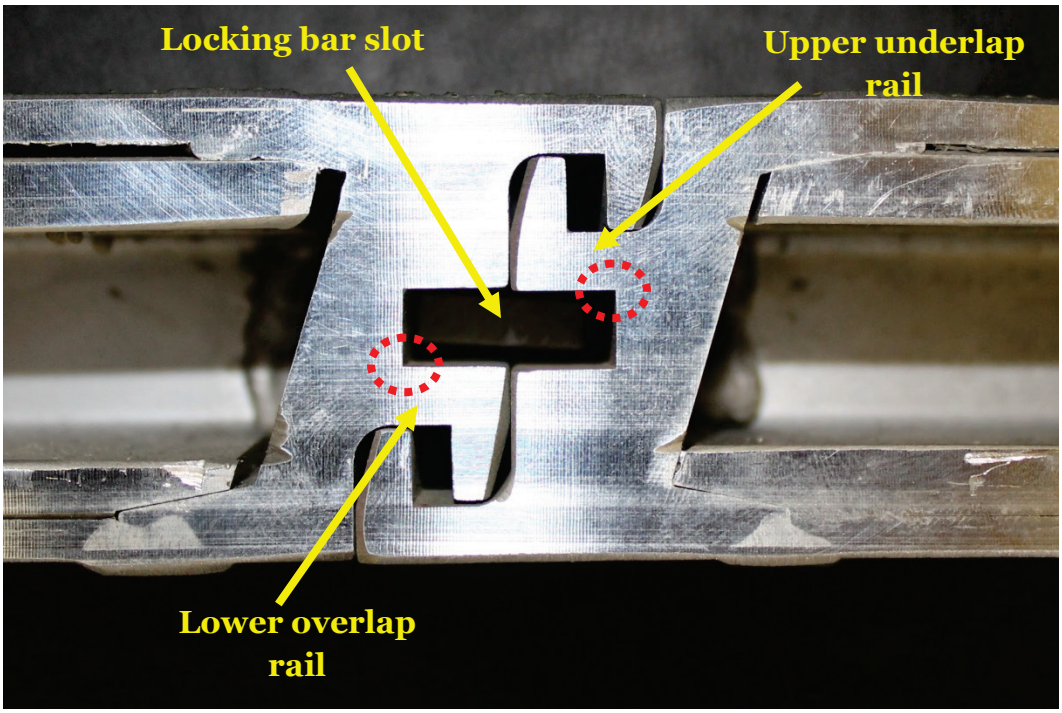

Figure 3. Crack initiation at lower overlap rail.

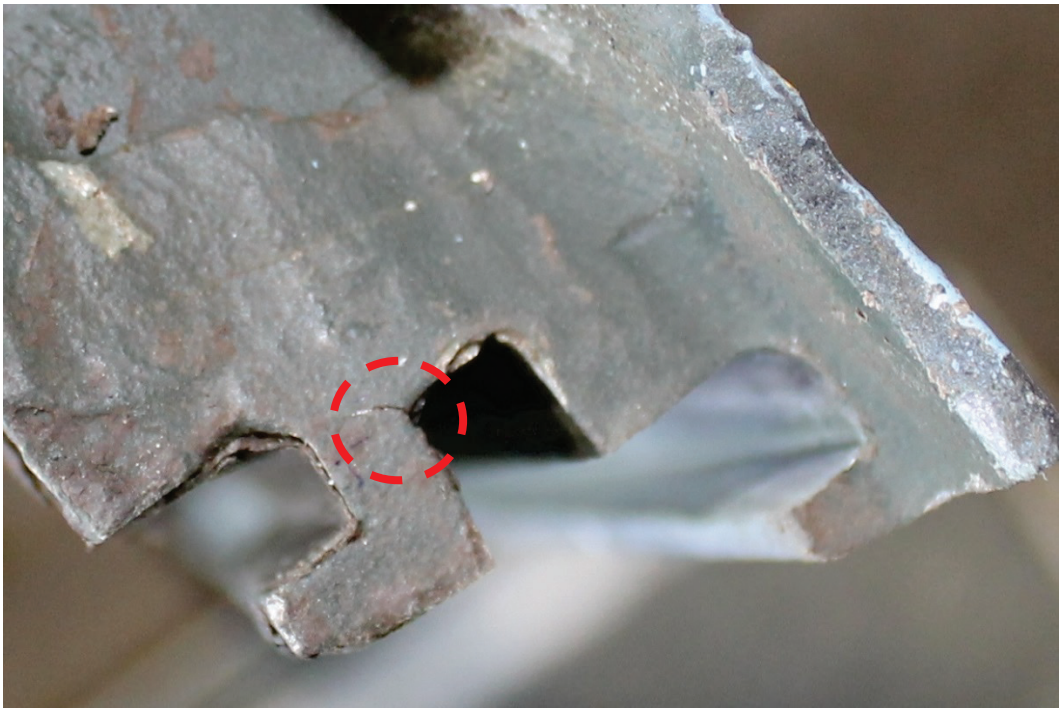

The die was recently corrected after an unknown period of producing the non-filleted design. Researchers questioned whether this fillet omission might have affected the performance of AM2 throughout the NAVAIR and AFCEC test program. Based on modeling results, it was assumed that a filleted corner would reduce stress concentrations at these locations and provide better fatigue life of the rails. Therefore, AFCEC sponsored an evaluation to quantify the difference in performance (if any) between an AM2 production without the filleted corners in the locking bar channel and a production lot with the filleted corners. Each test item was installed in the brickwork pattern. The results showed a significant increase in the performance life with the filleted corners. Further details of this test are reported by Garcia et al. (in preparation).

To provide additional insight on the performance of the recently corrected end connector design, the modified 2-1 lay pattern evaluation described in this report was conducted with AM2 panels having the filleted corners at the critical stress locations along the wheel path. Results of this test with the filleted design also represent the performance of future AM2 panel productions.

1.2 Objective and scope

The objective of the evaluation was to determine whether the modified 2-1 lay pattern could sustain more passes to failure than the original 2-1 lay pattern. A full-scale test section having a 36-in.-deep subgrade prepared to a CBR of 6 was surfaced with AM2 matting that consisted of filleted corners in the locking bar slot along the wheel path. The mat surface was subjected to simulated F-15E traffic. The results were compared against the baseline criteria for AM2 (Rushing and Tingle 2007) and the general performance exhibited by the original 2-1 lay pattern under F-15E traffic.

2 Materials

2.1 AM2 airfield mat

AM2 airfield mat was developed in the 1960s under a program sponsored by the Naval Air Engineering Center in Philadelphia, PA. Various versions of AM2 were tested under simulated aircraft loads at the U.S. Army Engineer Waterways Experiment Station in Vicksburg, MS, from 1961 through 1971, with major procurements beginning in 1965. The original AM2 mat has been modified through the years to address limiting structural concerns. The current production version of AM2 is Mod 5.

AM2 full panels are 2 ft by 12 ft by 1.5 in. and are fabricated from a single 6061-T6 aluminum alloy extrusion with end connectors welded to the 2-ft ends to form a complete panel. The core of the extruded panels is comprised of vertical stiffeners spaced 1.75 in. apart in the 12-ft direction. The mat is also made in half-panels to allow a staggered brickwork configuration. The panels are joined along the two 12-ft edges by a hinge-type male/female connection. The adjacent 2-ft ends are joined by an overlap/underlap connection secured by an aluminum locking bar. The panels are coated with an antiskid material to increase the surface friction. Pertinent properties of the AM2 mat are shown in Table 3.

The AM2 panels used for testing along the wheel path were manufactured in 2014 and supplied by ALFAB, Inc. AM2 panels used on the edges of the test surface were manufactured in October 2013 and were supplied by NAVAIR. Photographs of the delivered panels are shown in Figure 4.

Table 3. AM2 mat properties.

	Full-panel	Half-panel
Length (ft)	12	6
Width (ft)	2	2
Thickness (in.)	1.5	1.5
*Panel Weight (lbf)	145.5	74.4
*Unit Weight (lbf/ft^2)	6.1	6.3

Figure 4. NAVAIR F71 package (left) and ALFAB, Inc. AM2 bundles (right).

2.2 High-plasticity clay (CH) subgrade

The CH material used for subgrade construction was procured from a local source in Vicksburg, MS, and was subjected to the laboratory tests listed in Table 4. Classification data for the subgrade soil are shown in Figure 5. Moisture-density and CBR-moisture content relationships are shown in Figures 6 and 7, respectively. These data were used to determine the target moisture content and dry density required to obtain the target CBR of 6.

Table 4. Laboratory tests for Vicksburg Buckshot CH.

Test name	ASTM
Standard practice for classification of soils for engineering purposes (USCS)	D 2487
Standard test method for particle size analysis of soils	D 422
Standard test method for laboratory compaction characteristics of soil using modified effort	D 1557
Standard test method for cbr of laboratory compacted soils	D 1883
Standard test methods for liquid limit, plastic limit, and plasticity index of soils	D 4318

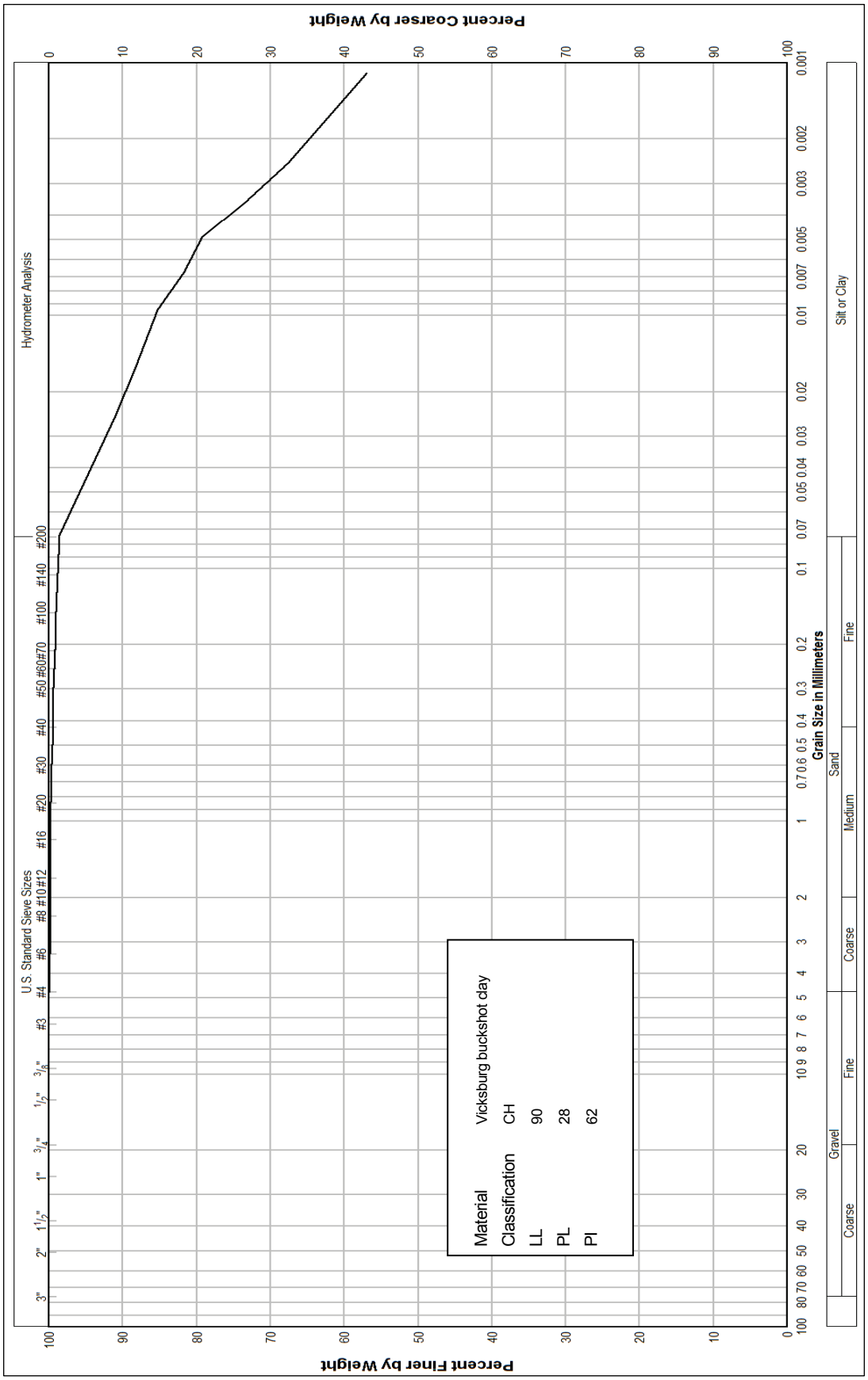

Figure 5. Gradation curve for Vicksburg Buckshot CH.

Figure 6. Dry density vs. moisture content for CH subgrade material.

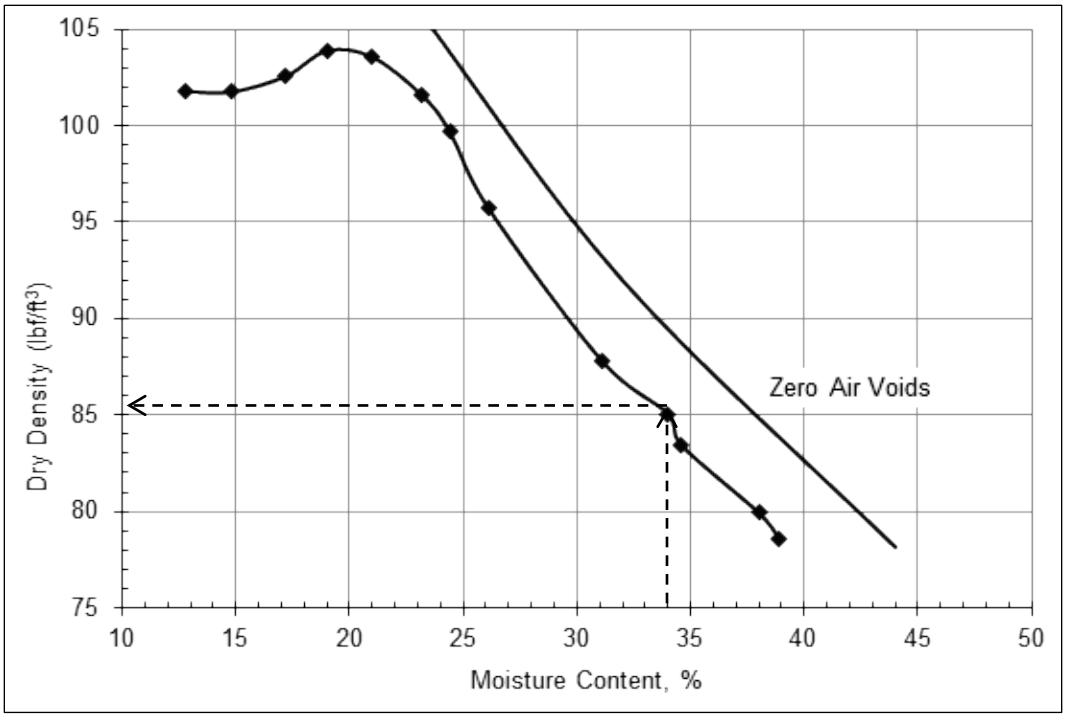

Figure 7. CBR vs. moisture content for CH subgrade material.

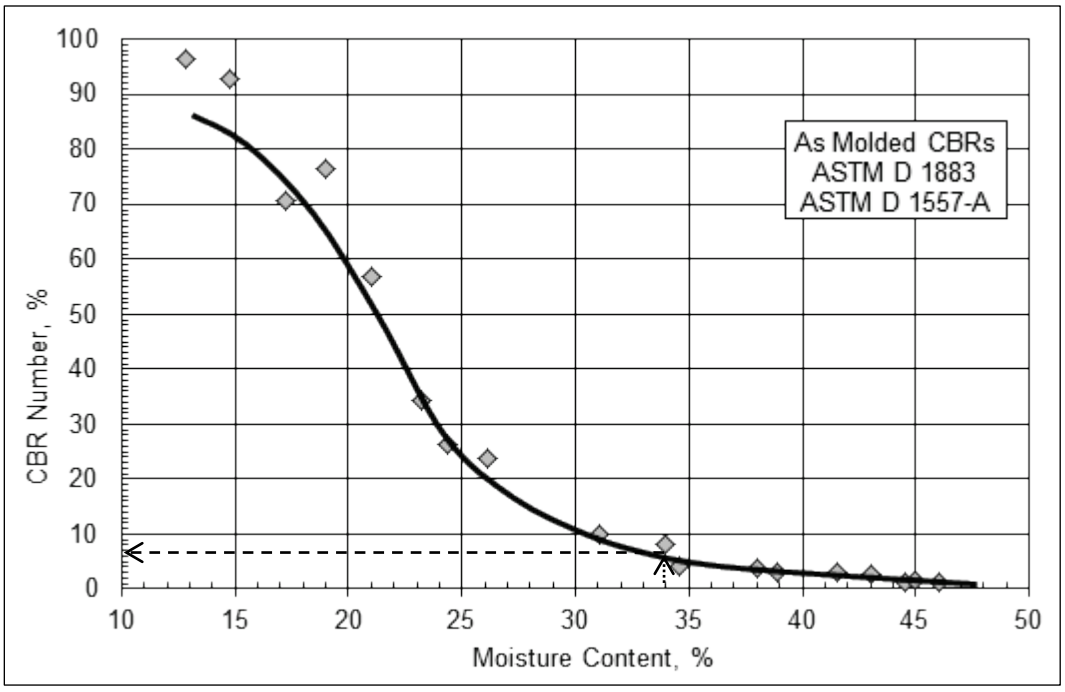

3 Experimental Program

3.1 Test section general description

A full-scale test section was constructed and trafficked under shelter in the Hangar 4 pavement test facility at ERDC. AM2 mat panels were placed directly over a 36-in.-deep CH subgrade prepared to a CBR of 6 over an existing silt foundation (ML), as shown in Figure 8. Polyethylene sheeting was placed between the silt foundation and the CH and along the walls of the subgrade pit to minimize moisture migration from the CH soil. A general layout of the test section along with panel designations is shown in Figure 9.

Each panel was identified with a number to track damage during trafficking. The matting surface was 36 ft wide by 42 ft long. The test had a 3.75-ft-wide lane designated for simulated F-15E traffic. Since a limited number of filleted AM2 panels were provided by Alfab, Inc., panels that were not subjected to traffic were supplied by NAVAIR (e.g., panel J3), which did not consist of filleted corners. Traffic was applied in a normally distributed wander pattern associated with the F-15E.

3.2 Test section construction

The following sections describe the construction of the foundation sub-grade and the AM2 mat installation. Field and laboratory soil testing data used to characterize the moisture, density, and bearing capacity in terms of CBR are also included.

Figure 8. Test section cross section.

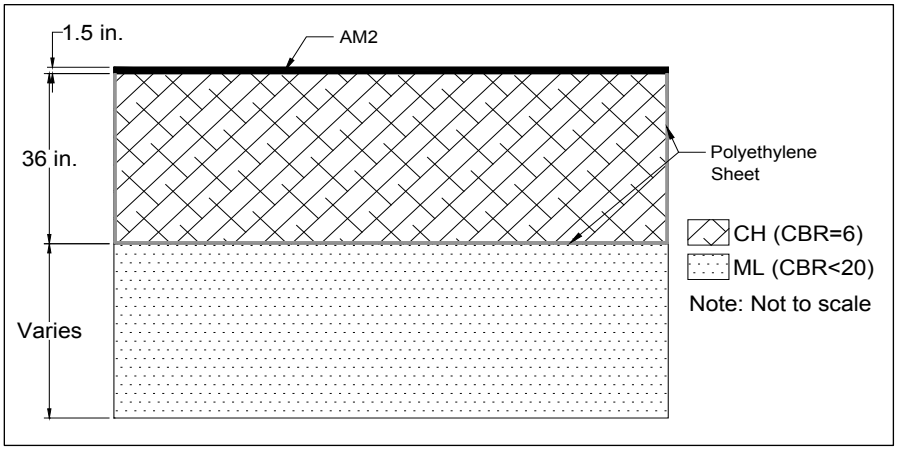

Figure 9. AM2 panel layout.

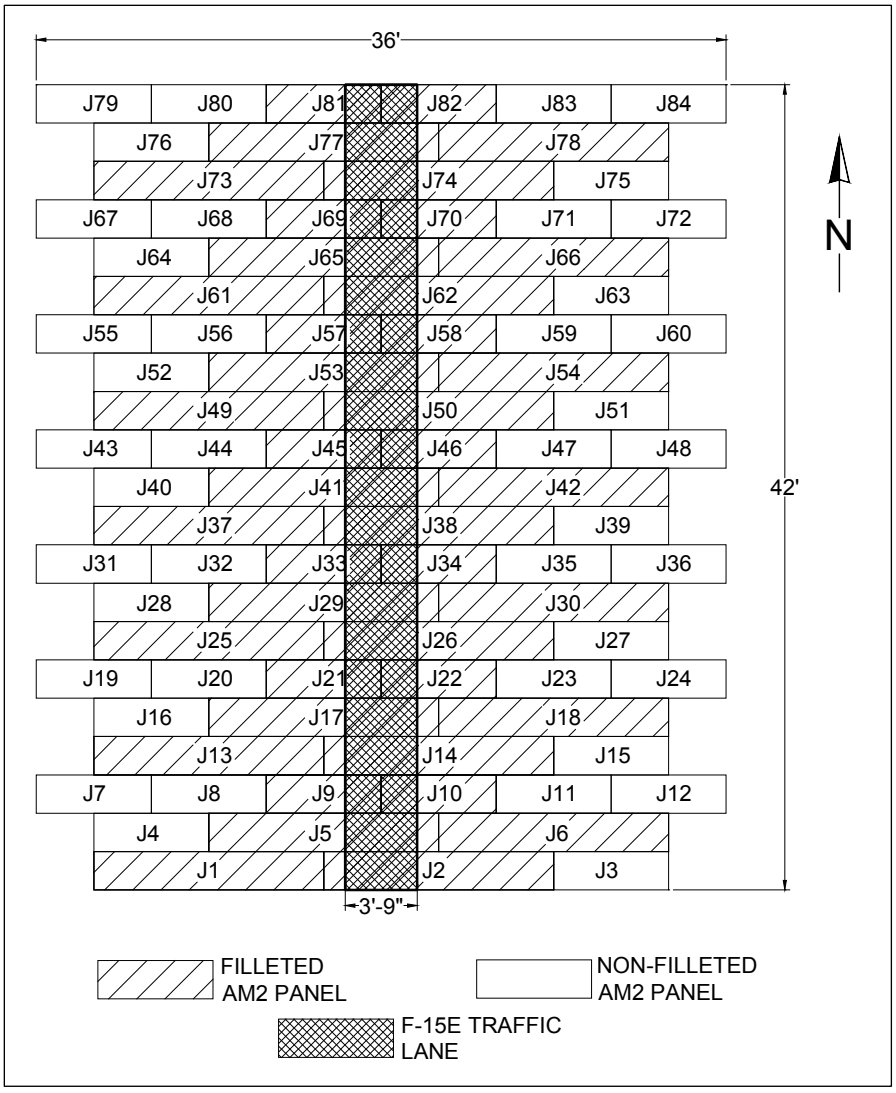

3.2.1 Subgrade construction and post-test forensics

The test section subgrade was built using in-place material from a previous AM2 test section constructed to a CBR of 6. Details of the construction of the previous mat evaluation are reported in Garcia et al. (in preparation). The original subgrade was constructed by excavating a 60-ft-wide by 42-ft-long test pit to a minimum 36-in. depth below the existing finished grade in Hangar 4 (Figure 10). The soil at the bottom of the excavation was a silt material (ML) having a CBR less than 20. The bottom and sides of the test pit were lined with impervious 6-mil polyethylene sheeting to minimize moisture migration from the 36 in. of new CH soil serving as the test section subgrade, as shown in Figure 10. Photographs of the construction process are shown in Figures 11 through 14.

Figure 10. Test section excavation (left) lined with impervious sheeting (right).

Figure 11. Pulverizing CH (left) and adding moisture (right).

Figure 12. Leveling (left) and compacting (right) CH.

Figure 13. Nuclear gauge (left) and sand cone (right) test.

Figure 14. Field CBR test.

For the evaluation discussed in this report, the upper 6 to 8 in. (approximately 1 lift) of an area 36 ft wide by 42 ft long of the existing test bed were removed and replaced with newly processed CH material. Post-test values from the previous evaluation 6 in. below the surface of the subgrade showed that the material retained its moisture and a CBR of approximately 6. It was assumed that the remainder of the subgrade depth retained its pretest values. Therefore, reconstruction of the entire depth was unnecessary.

The new CH material was processed at a nearby preparatory site by spreading it to a uniform 12-in. depth, pulverizing the material with a rotary mixer, adjusting the moisture content, pulverizing the material again, and stockpiling it, as shown in Figure 11. This was an iterative process necessary to achieve a uniform distribution of moisture throughout the material. Once the CH had been processed to the target moisture content, it was placed in

the test section, spread by a bulldozer in an 8-in. lift, and compacted with a pneumatic roller to a thickness of 6 in., as shown in Figure 12. The new compacted lift was subjected to the test methods listed in Table 5 to verify that target values had been met (Figures 13 and 14). In situ CBR, laboratory oven moisture, nuclear gauge, and dynamic cone penetrometer tests were performed at (or with samples from) stations 10, 20, and 30 along the centerline. The remaining methods listed in Table 5 were conducted at offset locations.

Table 5. Field tests on each constructed lift.

Test Name	Test Designation	Pre-test	Post-test
Standard Test Method for Density of Soil in Place by the Drive Cylinder	ASTM D 2937	X	
Standard Test Method for In-Place Density and Water Content of Soil and Soil-Aggregate by Nuclear Methods (Shallow Depth)	ASTM D 6938	X	X
Standard Test Method for Density and Unit Weight of Soil in Place by the Sand Cone Method	ASTM D 1556	X	
Standard Test Method for Laboratory Determination of Water Content of Soil and Rock Mass	ASTM D 2216	X	X
Standard Test Method for Use of the Dynamic Cone Penetrometer in Shallow Pavement Applications *	ASTM D 6951	X	X
Standard Test Method for Determining the California Bearing Ratio of Soils (ERDC 1995)	CRD-C654-95	X	X

*Conducted after last lift was compacted.

Once trafficking was completed, posttest forensics were conducted at the same locations to determine the depth of subgrade that might have undergone gradual drying and possible densification under traffic. Some increase in CBR was expected because of thixotropic properties of clay structures and gradual drying and densification during trafficking. Based on historic testing data, increases of less than 5 CBR at the surface and increases of less than 3 CBR at a depth of 6 in. are common and therefore acceptable (Rushing and Tingle 2007; Rushing and Torres 2007; Rushing et al. 2011; Garcia et al. 2012; Rushing et al. 2012).

Subgrade properties prior to installing mat and after completing traffic are shown in Table 6. Changes in CBR on the surface and 6 in. below the surface were within +1 and -0.5 CBR. Additional testing below 6 in. was not required since the changes were within acceptable limits.

Table 6. Average in situ properties of the subgrade.

Test Depth	Drive Cylinder		Sand Cone		Nuclear Gauge			CBR		
	Moisture %	Dry Density (lbf/ft³)	Moisture %	Dry Density (lbf/ft³)	Wet Density (lbf/ft³)	Dry Density (lbf/ft³)	Moisture %	Moisture %	In Situ CBR	Δ CBR
PRETEST										
Surface [a]	30.8	87.3	31.3	92.8	117.6	90.7	29.5	32.2	5.7	-
6 in. [b]	32.5	87.1	33.0	92.2	119.2	92.2	29.4	34.5	6.3	-
12 in. [c]	35.5	86.4	34.9	90.3	116.1	89.1	30.3	34.5	5.5	-
18 in. [c]	32.4	86.0	31.9	95.9	115.2	88.3	30.5	32.1	6.2	-
24 in. [c]	32.4	86.0	31.9	95.9	116.8	90.3	29.4	33.5	5.9	-
30 in. [c]	33.7	84.7	33.7	89.7	115.4	88.4	30.5	33.2	6.2	-
POST TEST										
Surface	-	-	-	-	117.9	90.1	30.9	33.7	6.7	1.0
6 in.	-	-	-	-	116.6	88.8	31.3	34.1	5.8	-0.5

[a] New compacted lift

[b] Measured after removing top lift of previous mat evaluation

[c] Average pretest values of previous mat evaluation

3.2.2 AM2 mat installation

The AM2 airfield mat system was placed on the surface of the prepared test section subgrade by an experienced crew. The mat bundles were placed on the test section with a forklift, and the individual panels were carried by two men and placed into position.

The first mat panel was placed flat on the ground with the long dimension perpendicular to the direction of traffic and with the male hinge connector facing north. The second panel was positioned adjacent to the 2-ft end of the first, allowing the overlapping end connector of the second panel to drop into position over the underlapping end connector of the first panel. A rectangular slot was formed between the two end connector rails, and an aluminum locking bar was inserted into the slot, as shown in Figure 15. This locking bar prevented the ends of the mat panels from separating. This process was continued until the first row was installed.

Figure 15. Insertion of aluminum locking bar between adjacent panels.

For the second row, the female hinge connector was attached to the male hinge connector of panels from the first row, and the panel was pivoted into place, as shown in Figure 16. The next panel was installed by attaching the female hinge connector to the male hinge connector of panels in the first row and allowing the overlapping end connector rail to pivot over and connect to the underlapping end connector rail of the adjacent panel. An aluminum locking bar was inserted into the space provided to keep the panels from separating.

For the third row, a half-panel was marked at the midsection and half of the female hinge was attached to a panel in row 2. The other half of the panel extended 3 ft east of the rows already installed. Once row 3 was completed, the half-panel located on the other end extended 3 ft west of the edge of rows 1 and 2 (Figure 9). This process was repeated until the entire mat test section was assembled in a modified 2-1 pattern.

Once assembly was complete, full-panels of AM2 were installed along the ends of the traffic lanes to facilitate the entrance and exit of the test vehicles. Male keylocks were attached to the female hinge connector of the panels in the first row to facilitate ramp installation, as shown in Figure 17. A photo of the assembled test item is shown in Figure 18. Once the mats had been installed, 1,000-lb steel blocks were placed along the edges of the test section to anchor the mats and simulate the resistance to movement provided by a large expanse of matting.

Figure 16. Installation of AM2 panels on the test section subgrade.

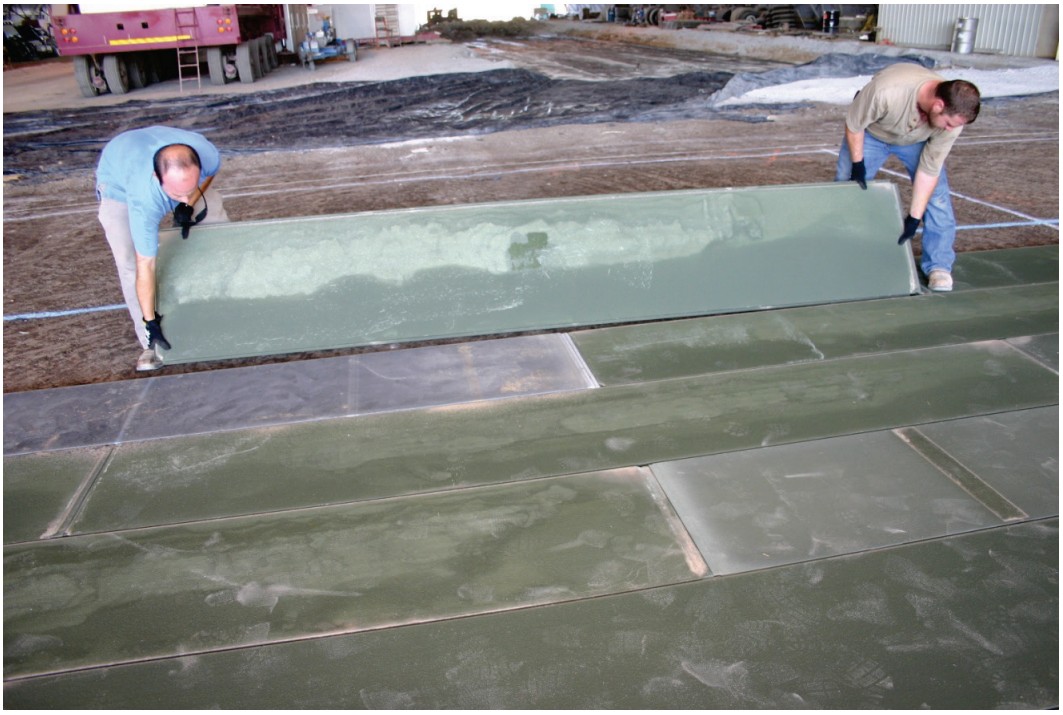

Figure 17. Typical installation of male keylock.

Figure 18. Assembled mat surface.

3.3 Traffic application

A specially designed single-wheel load cart was used to simulate F-15E aircraft traffic. The load cart was equipped with a 36-in. by 11-in., 30-ply tire inflated to 325 lbf/in.^{2} and loaded such that the test wheel was supporting 35,235 lb. The F-15E load cart was equipped with an outrigger wheel to prevent overturning and was powered by the front half of a U.S. Army 2.5-ton transport truck, as shown in Figure 19.

A normally distributed pattern of simulated traffic was applied in a 3.75-ft-wide traffic area for the F-15E test item, as shown in Figure 20. The traffic area was broken into five lanes that were designed to simulate the traffic distribution pattern, or wander width, of the main landing gear wheel on a mat surface when taxiing to and from an active runway. The width of each lane corresponded to the measured contact width, 9 in., of the F-15E tire when fully loaded and not to the overall published tire width of 11 in. The normally distributed traffic patterns were simplified for ease-of-use by the load cart operator. Traffic was applied by driving the load cart forward and then backward over the length of the test item and then shifting the path of the load cart laterally approximately one tire width on each forward path. Tracking guides were attached to assist the driver in shifting the load cart the proper amount for each forward path. This procedure was continued until one pattern of traffic was completed. One pattern resulted in 16 passes, or 4 coverages.

Figure 19. F-15E test load cart.

Figure 20. Plan view showing F-15E normally distributed traffic lanes.

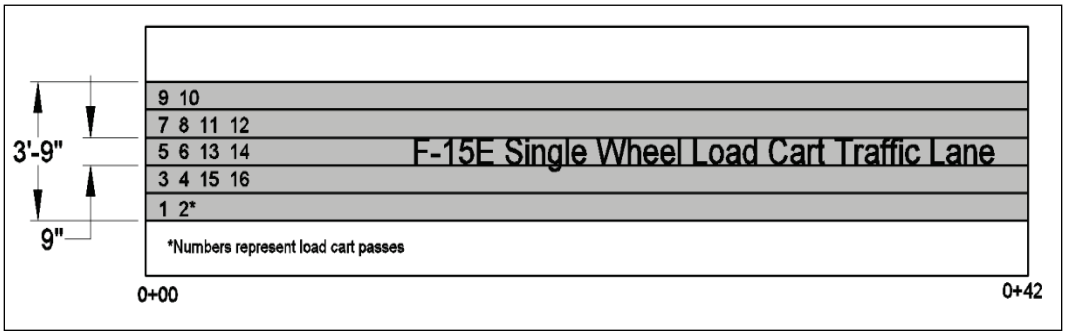

3.4 Data collection

Data collection included robotic total station measurements of centerline profiles, cross sections, and elastic deflection. Data were collected at the pass levels shown in Table 7. The data collection layout is shown in Figure 21. The mat surface was inspected for damage periodically during traffic.

Table 7. Data collection pass levels.

Total Passes	Profile	Unloaded Cross Sections	Loaded Cross Sections	Elastic Deflection
Pretest Subgrade	X	X		
0	X	X	X	
10	X	X	X	
16	X	X	X	X
32	X	X	X	X
48	X	X	X	X
112	X	X	X	X
240	X	X	X	X
496	X	X	X	X
1008	X	X	X	X
1520	X	X	X	X
1728	X	X	X	
2032	X	X	X	X
2850	X	X	X	X
Posttest Subgrade	X	X		

3.4.1 Centerline profile

Elevation data collected along the traffic centerline on the pretest subgrade, on the mat at scheduled pass levels, and on the posttest subgrade after removing the mat (Figure 22) are labeled "centerline profiles" in this report. Robotic total station elevation data were collected at 6-in. intervals on the subgrade and at 1-ft intervals on the mat surface.

3.4.2 Unloaded cross sections

Elevation data collected transverse to the direction of traffic at the locations labeled A1, A2, and A3 on the pretest subgrade, on the mat at scheduled pass levels, and on the posttest subgrade after removing the mat, are called "cross sections" in this report. The locations of perpendicular lines A1, A2, and A3 were selected near the quarter-points of the test items to characterize the average performance while avoiding potential end effects associated with boundary conditions at the ends of the test sections. Robotic total station elevation data were collected at 6-in. intervals on the subgrade. On the mat surface, data were collected at 1-ft intervals (Figure 23).

Figure 21. Data collection layout.

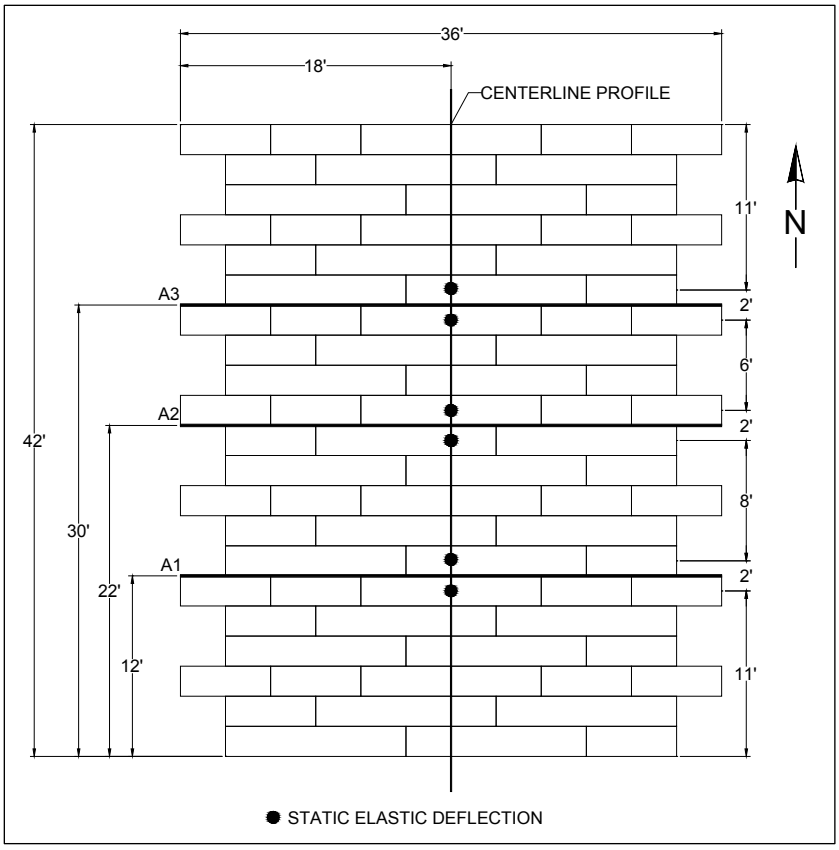

Figure 22. Typical survey of subgrade.

Figure 23. Surveying unloaded (left) and loaded (right) cross section.

3.4.3 Loaded cross sections

In an attempt to measure the permanent deformation of the subgrade underneath the mat surface, a forklift carrying two 2,000-lb lead blocks was parked on the mat surface adjacent to each cross section, and elevation data were once again recorded at the same intervals (Figure 23). The wheel load applied was approximately 6,000 lb. These data are noted as "loaded cross sections" in this report. The goal of the load application was to deflect the mat enough to contact the subgrade but not so much as to induce elastic deflections in the subgrade.

3.4.4 Elastic deflection

Elastic deflection was measured at the pass levels in Table 7 by taking robotic total station readings at the locations shown in Figure 21, both on the unloaded mat surface and immediately adjacent to the tire of the load cart parked on the same locations (Figure 24). The quarter point (3 ft from end) of three panels and the end connector joint at three locations were specifically chosen to represent the least and most critical positions of the mat, respectively.

3.5 Failure criteria

The failure criteria established were either (1) 10 percent mat breakage or (2) the development of 1.25 in. of permanent surface deformation for the F-15E. These failure criteria were developed based upon previous testing of airfield matting and USAF requirements. Failure criteria values were recorded and monitored for compliance.

Figure 24. Elastic deflection measurement.

3.5.1 Mat breakage

Mat breakage percentages were calculated by dividing the area of the failed panel (or half-panel) by the total area influenced by the simulated traffic application in the assembled test item. Individual panels were considered failed if observed damage posed a significant tire hazard or caused instability of the load cart. Tire hazards were defined as damage that could not be reasonably maintained by simple field maintenance procedures. A typical example was a top skin tear in excess of 10 in., representing significant structural damage to the surface skin with sharp edges that might endanger an aircraft tire.

3.5.2 Permanent deformation

The permanent surface deformation limit of 1.25 in. is based on roughness limitations for the F-15E aircraft. An abrupt change in elevation or the development of a rut in the wheel path greater than the allowable values may exceed roughness limits. The rut depth limit is required, since many connecting taxiways and aprons intersect at 90 deg, and crossing perpendicular to a preformed rut may cause an abrupt change in elevation, exceeding aircraft limits. Permanent surface deformation was determined from robotic total station elevation measurements of cross sections and

centerline profiles. Each of the following data collection categories was analyzed for compliance with the failure criterion:

1. centerline profile deformation,
2. unloaded surface deformation, and
3. loaded surface deformation.

3.5.2.1 Centerline profile deformation

The difference in elevation one to two stations apart (1 ft to 2 ft apart) was analyzed from plots of the centerline profile data to determine whether an abrupt change in elevation reached failure limits during trafficking.

3.5.2.2 Unloaded surface deformation

Unloaded surface deformation was determined from data collected according to the procedures described in Section 3.4.2. The maximum deformation at each location was determined as the difference in elevation from the average height of the elevated material on each side of the trough to the deepest point in the bottom of the trough. Measurements were averaged to obtain a single value for comparison to the failure criterion.

3.5.2.3 Loaded surface deformation

Loaded surface deformation was determined from data collected according to the procedures described in Section 3.4.3. The maximum deformation at each location was determined as the difference in elevation from the average height of the elevated material on each side of the trough to the deepest point in the bottom of the trough. Measurements were averaged to obtain a single value for comparison to the failure criterion.

4 Test Results

4.1 Mat behavior (visual observations)

Trafficking began on 27 October 2014. Figure 25 shows the layout of the failed panels as noted by visual observation in the test section. The accumulation of mat damage and mat breakage throughout trafficking and the damage noted after removing panels from the subgrade surface are summarized in Table 8.

Figure 25. Layout of failed panels.

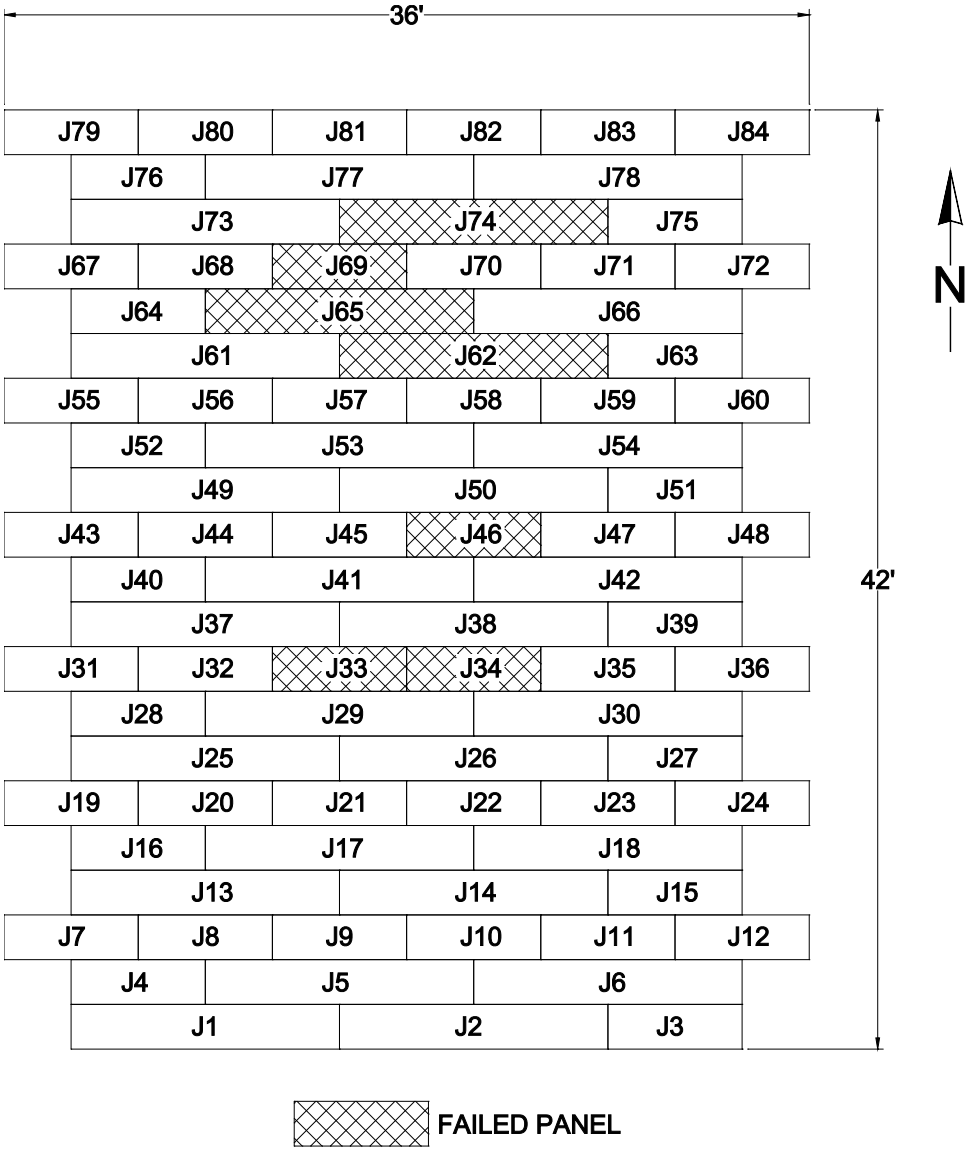

Table 8. Mat damage.

Pass number	Panel number	Description of damage	Cumulative failed panels*	Cumulative mat breakage, %
496	All panels with joint along centerline	0.125-in. corner curl at south corner	-	-
1008	J81, J82, J69, J70	Corner curl more severe, increased to 0.1875 in.	-	-
	J45, J21	Corner curl increased to 0.25 in., developed minor cracking on surface	-	-
1202	J46	Top skin tear, 3.25 in. long	-	-
	J81, J82	Corner curl increased to 0.25 in., developed minor cracking on surface	-	-
1286	J34	Top skin tear, 3 in. long	-	-
	J46	Skin tear length increased to 4 in.	-	-
	J45	Top skin tear, 1.5 in. long	-	-
1520	J34	Top skin tear, 5.5 in. long	-	-
	J33	Top skin tear, 2 in. long	-	-
	J46	Skin tear length increased to 5 in.	-	-
	J45	Minor crack at weld on south edge	-	-
	J57	Minor crack at weld on south edge	-	-
	J9, J10	Corner curl more severe, increased to 0.1875 in.	-	-
1560	J29, J30	Corner curl became tire hazard. Hit with hammer for maintenance	-	-
1644	J46	Skin tear length increased to 11 in. Cut for maintenance.	1 (H)	1.2
	J45 – J46	Popping heard at joint. No crack visible from surface. Separation of joint noted in south area	-	-
	J33, J34	Small piece of south corner of top skin chipped off	-	-
1718	J46	Upper underlap rail broke. Skin tear length increased to 24 in.	-	-
	J34	Skin tear length increased to 7.5 in.	-	-
	J33	Skin tear length increased to 8.5 in.	-	-
1728	--	Failure at J46 became tire hazard. Metal plate placed over J46 – J45 to bridge over damage.	-	-
2032	J45	Skin tear length increased to 7 in.	-	-
	J33	Skin tear length increased to 13 in.	2 (H)	2.4
	J34	Skin tear length increased to 13.5 in.	3 (H)	3.6
2200	J33, J34	Skin tear cut for maintenance	-	-

Pass number	Panel number	Description of damage	Cumulative failed panels*	Cumulative mat breakage, %
2424	J74	Core crushing in traffic area (22 in. wide by 5 in. long). Top flange of female hinge sheared from top skin (22 in. long)	4 (F)	6.0
	J34	Skin tear length increased to 15 in.	-	-
	J33	Skin tear length increased to 16.5 in.	-	-
	--	Rubber mat placed on J74 to cover tire hazard	-	-
2638**	J65	Core crushing in traffic area (9 in. wide by 6.5 in. long)	5 (F)	8.3
	J62	Core crushing in traffic area (12 in. wide by 3 in. long)	6 (F)	10.7
	J74	Crushed core area increased to 23 in. wide by 17.5 in long. Top flange sheared length increased to 34 in.	-	-
2850	J69	Joint with J70 separating. Lower overlap rail may have broken	-	-
	J74	Two cracks developed on top skin. One near north area of panel (20 in. long); the other near south area of panel (42 in. long). Crushed core area increased (33 in. wide)	-	-
	J65	Crushed core area increased (23 in. wide by 13 in. long)	-	-
	J62	Crushed core area increased (24 in. wide by 12 in. long)	-	-
	J34	Skin tear length increased to 20 in.	-	-
	J33	Skin tear length increased to 22.5 in.	-	-
	J46	Skin tear length increased to 25 in. (with metal plate on it)	-	-
	J45	Skin tear length increased to 9 in. (with metal plate on it)	-	-
Post Test (2,850)	J81	1.75 in. crack on surface of upper overlap rail, starting at north edge (male hinge edge)	-	-
	J77	Bowed in traffic area	-	-
	J74	Two cracks on bottom skin: One was 33.5 in. long and 18 in. offset from north edge; the other was 39 in. long and 6 in. offset from north edge. Crack along face of female hinge, 64 in. long	-	-
	J69	Lower overlap rail broke length of 16.5 in., starting at north edge. Surface of upper overlap rail had 2-in.-long crack, starting at north edge	7 (H)	11.9

Pass number	Panel number	Description of damage	Cumulative failed panels*	Cumulative mat breakage, %
	J70	Upper underlap rail broke a length of 10 in. long, starting at south edge		
	J65	Crack on bottom skin, 29 in. long. The crack was offset from north edge about 18 in.	-	-
	J62	Two cracks on bottom skin: One was 17 in. long and offset 6.5 in from north edge. The other was 37.4 in. long and offset 9.5 in. from north edge	-	-
	J50	Crack along face of female hinge 3.5 in. long	-	-
	J22	Upper underlap rail broke length of 1 in., starting at south edge	-	-
	J14	Crack along face of female hinge, 12 in. long	-	-
	J9	Lower overlap rail broke length of 1.5 in., starting at south edge	-	-

* (H) = half panel ; (F) = full panel

** Test section failed due to mat breakage > 10%

The most common failure mechanisms were top skin tearing greater than 10 in. and core crushing. The most common damage was minor stop skin tearing and corner curls. Top skin tears occurred in panels with their end connector in the traffic area. A top skin tear typically began at (or near) the south edge of the end connector weld and propagated along the top flange of the female hinge. Examples are shown in Figure 26. If a top skin tear reached a point where it was posing a risk to the load cart tire, it was cut for maintenance. Skin tears greater than 10 in. were difficult to maintain, and traffic had to be stopped frequently for maintenance. Therefore, if the length of the top skin tear reached more than 10 in., the panel was considered failed. Top skin corner curls occurred at the south corner of panels with their end connector along the centerline. They occurred before top skin tearing developed and were hammered down if they posed a risk to the tire.

Figure 26. Top skin tear on J46 (left) and J33 (right).

Four panels had breakage at the end connector: two at the upper underlap rail and two at the lower overlap rail. When a rail failure occurred, separation was noted at the adjoining panels as the load cart passed over the joint. Upper underlap rail failure was confirmed when a crack could be seen at the rail from the surface. Examples are shown in Figures 27 and 28. J70 was partially broken at the upper underlap rail, and J9 was partially broken at the lower overlap rail (Figure 28), but the length of breakage in these two panels was 10 in. and 1.5 in., respectively. Since these lengths were less than half the length of the rails, J70 and J9 were not considered failed.

Figure 27. Upper underlap rail breakage at J46 (left) and J70 (right).

Figure 28. Lower overlap rail breakage at J69 (left) and J9 (right).

After 1,728 passes, the skin tear and the upper underlap rail failure at J46 were posing serious risks to the load cart tire. Since it was important to continue traffic until mat breakage failure was achieved, a metal plate was placed over J46 and J45 to bridge over the damaged area (Figure 29).

Core crushing was documented in three panels. This failure mechanism is evident through dishing observed on the surface, as shown in Figure 30. Panel J74, which was the first to fail by core crushing, also sheared at the female hinge, creating a severe tire hazard. A rubber mat was placed over the panel (Figure 29) to cover the damaged area and to continue traffic.

Mat breakage failure was reached after 2,638 passes when 10.7 percent of the test item was documented as failed. Traffic was concluded after 2,850 passes, and the panels were removed from the test subgrade. After the panels were removed from the test section, panels where core crushing had occurred were noted to have cracks on the bottom skin (Figure 31).

Figure 29. Metal plate placed on J46/J45 (left) and rubber mat placed on J74 (right).

Figure 30. Core crushing in J74 (left) and J62 (right).

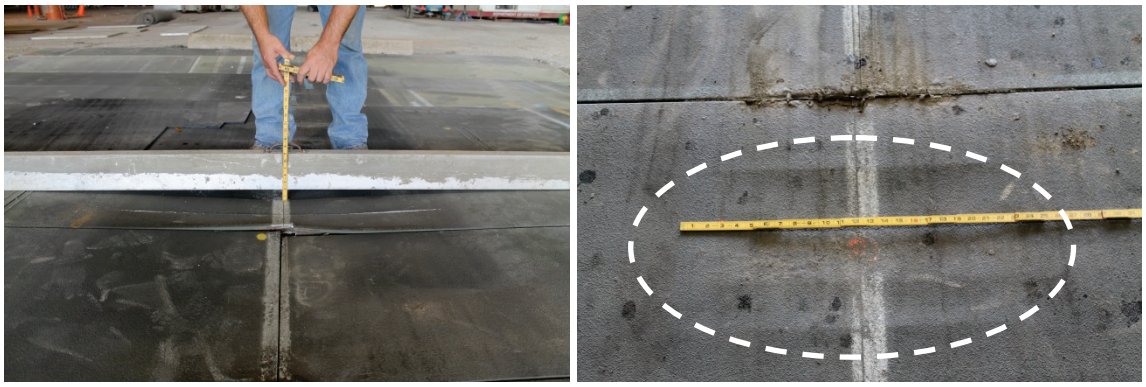

Figure 31. Cracks on bottom skin of J65 (left) and J62 (right).

4.2 Permanent deformation

The pre-traffic data were subtracted from all subsequent data collected after trafficking began to normalize the data and show only the changes caused by trafficking. Plots of the centerline profile data, as determined from robotic total station recordings, are shown in Figures 32 and33. When determining the maximum roughness value in each item, boundary conditions were ignored (i.e., first and last two stations along the centerline in Figures 32 and 33). This was done because of the different properties at the interface of the test section subgrade and the stronger surrounding material. Stations 16, 22, and 31 to 38 were areas of panel end connector rail failure, severe skin tears, or core crushing, and are represented as deep depressions in the subgrade and the mat surface. These were disregarded when analyzing the profile, since they were associated with mat breakage and not necessarily with the system's ability (or inability) to prevent excessive roughness.

Plots of the average cross-section elevation data, collected along lines A1, A2, and A3, are shown in Figures 34-36. Table 9 summarizes important deformation values determined from all the plots for comparison to the failure criterion. Note that after failure of panel J46, which was located at cross section A2, material rearrangement and buildup occurred beneath and around line A2. This affected any data collected along line A2 for the remainder of the test, giving an unrealistic measure of the deformation on the mat surface and the subgrade. Therefore, measurements shown in Figures 34-36 after pass 1,644 were the average of data collected along lines A1 and A3.

Figure 32. Subgrade centerline profile after 2,850 passes.

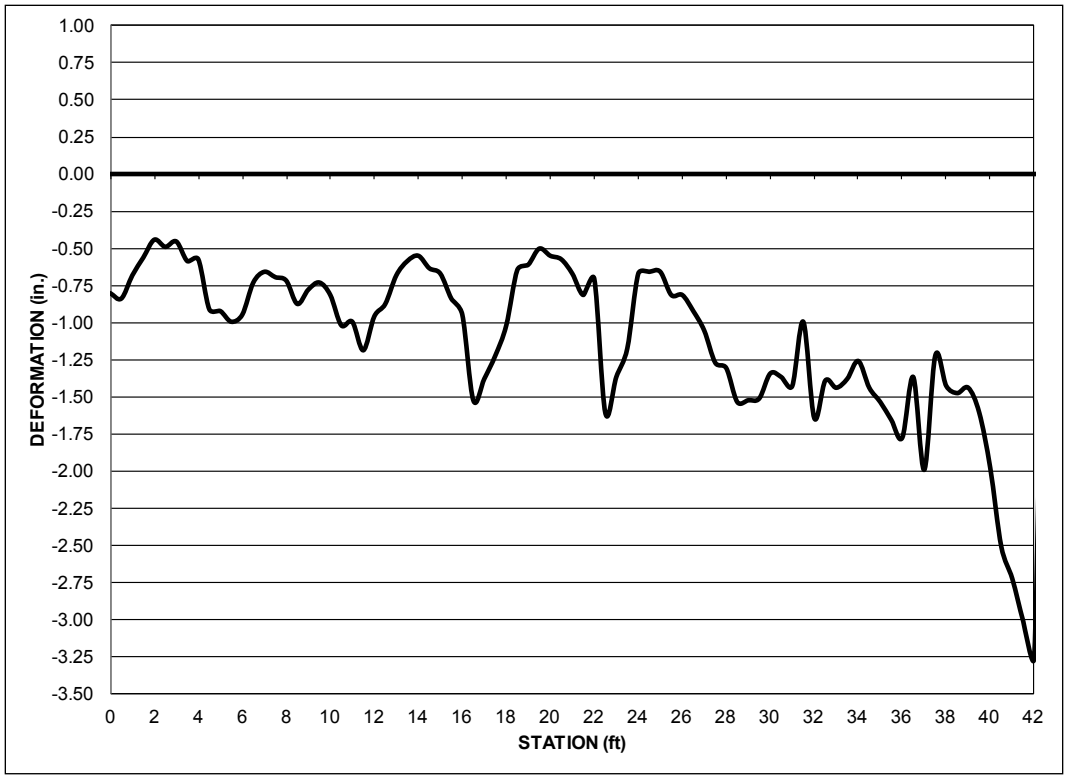

Figure 33. Centerline profile on the mat surface.

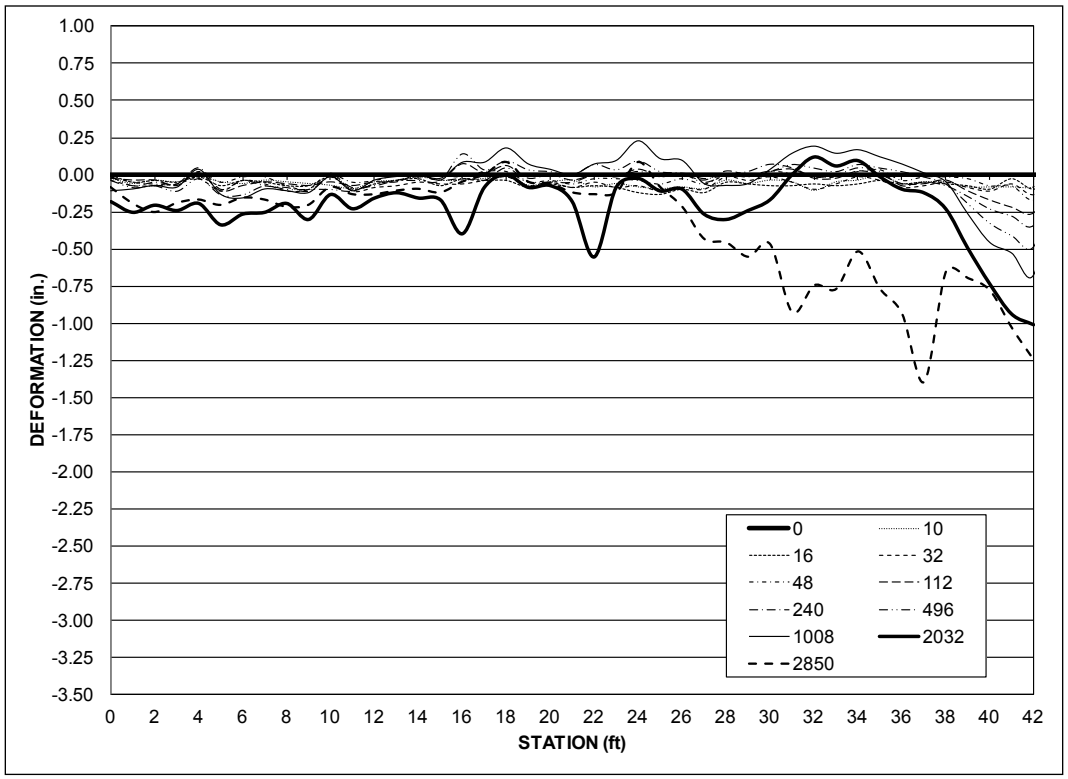

Figure 34. Average deformation on the subgrade after 2,850 passes.

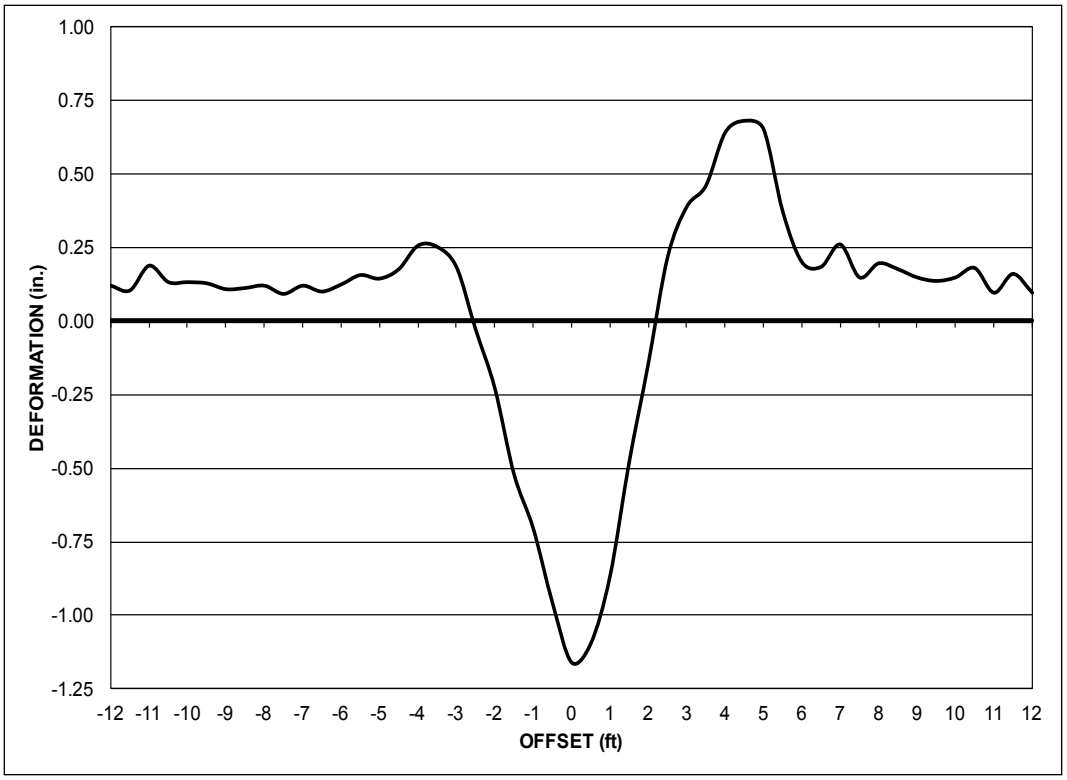

Figure 35. Average deformation on the unloaded mat surface at different pass levels.

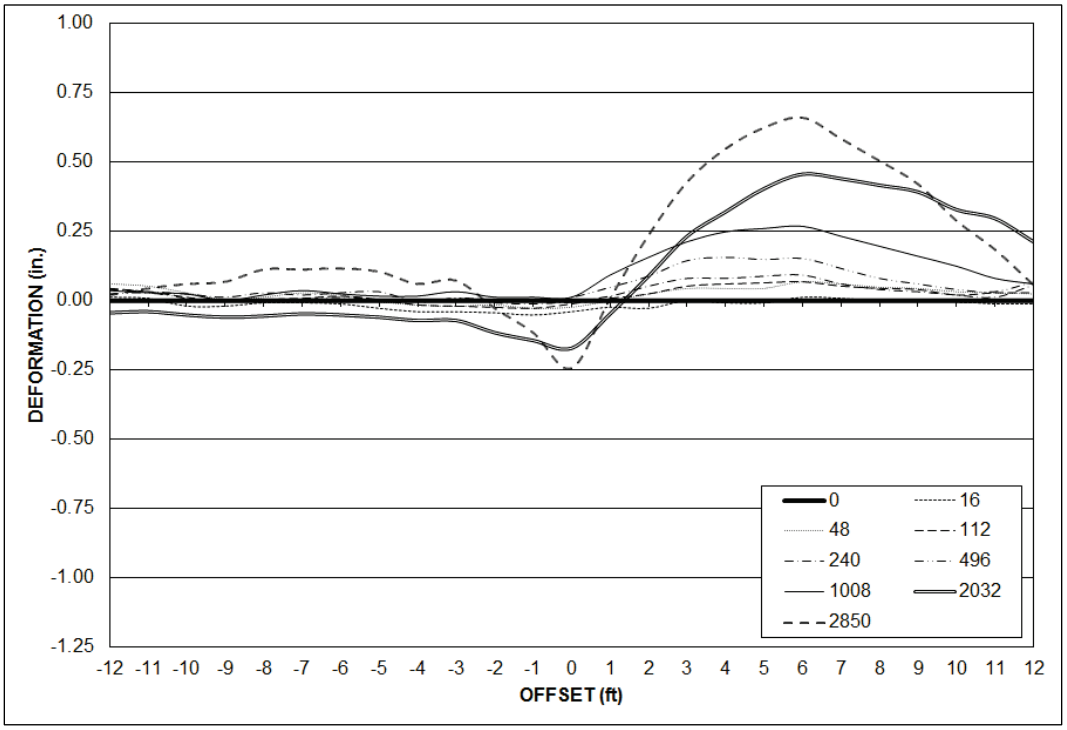

Figure 36. Average deformation on the loaded mat surface at different pass levels.

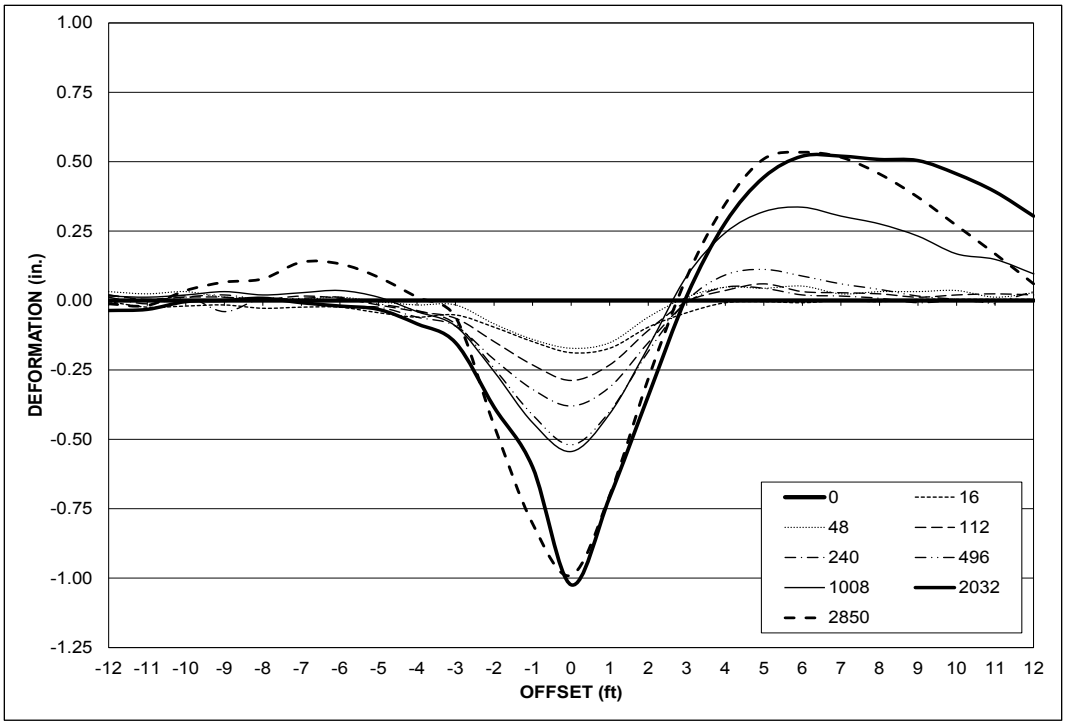

Table 9. Permanent deformation values at different pass levels.

Pass number	1,008	2,032	2,850
Subgrade profile max abrupt change in elevation (in.)	-	-	0.46
Mat surface profile max abrupt change in elevation (in.)	0.17	0.19	0.13
Subgrade permanent deformation (in.)	-	-	1.74*
Loaded deformation on mat surface (in.)	0.74	1.01*	1.34*
Unloaded deformation on mat surface (in.)	0.20	0.32*	0.66*

*These values are an average of measurements at A1 and A3.

4.3 Elastic deflection

The difference between the loaded (immediately adjacent to the tire of the load cart) and the unloaded elevations at the locations shown in Figure 21 represents the elastic deflection, or rebound, of the mat and the subgrade at each location. The measurements determined from readings taken at the quarter point (3 ft from end) of the three panels were averaged to give a final elastic deflection value. The same was done for measurements determined from readings taken at three joints. The average of these two values was also calculated. One number was reported for each condition at each pass level in Table 7. The results are shown in Figure 37. Note that measurements after pass 1,644 (failure of J46) represent the average of data collected near stations A1 and A3.

Figure 37. Elastic deflection.

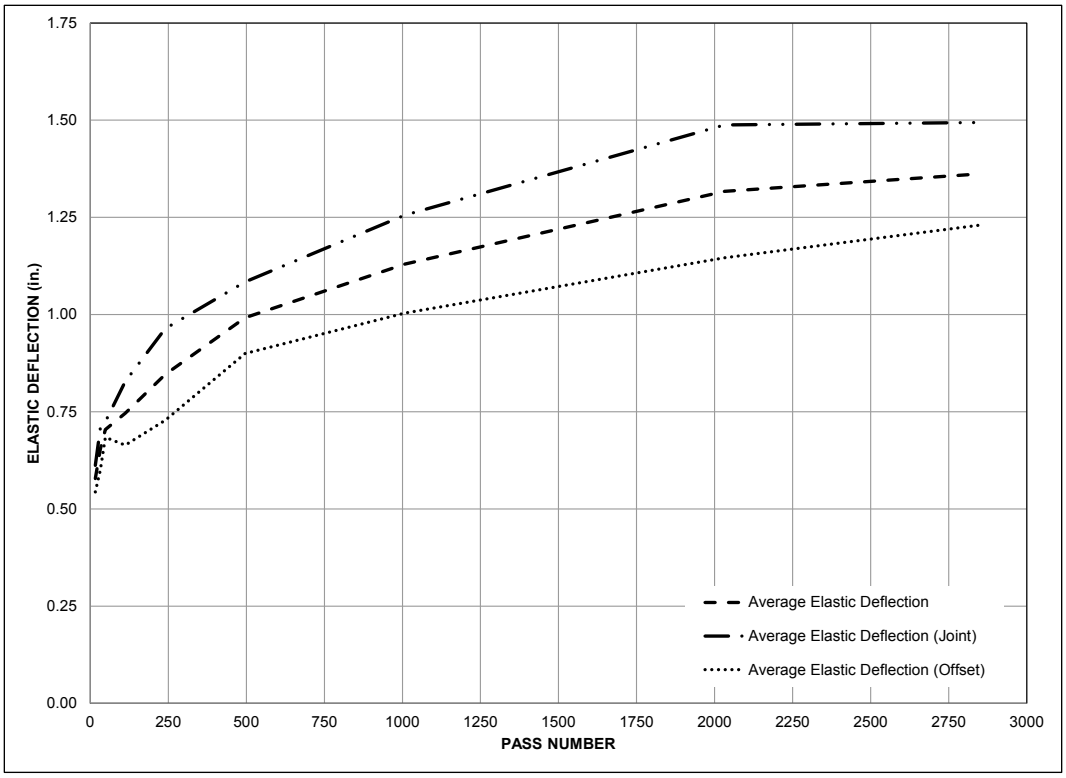

5 Analysis of Results

5.1 Mat breakage

The test section sustained 2,638 passes of simulated F-15E aircraft traffic before failure by mat breakage. The number of occurrences of the different failure mechanisms is provided in Table 10. All have been generally reported by Rushing and Tingle (2007), Rushing and Torres (2007), Rushing et al. (2008), Rushing and Mason (2008), and Garcia and Rushing (2013) in AM2 when trafficked over weak subgrade conditions.

Table 10. Frequency of mat failure mechanisms.

Failure type	Number of panels
Broken upper underlap rail	1*
Broken lower overlap rail	1
Top skin tear >10 in.	3
Core crushing	3

*J46 failed by top skin tear > 10 in. before upper underlap rail broke.

Rail breakage is the most common failure mechanism that occurs in AM2 panels when trafficked on soft soil. However, the frequency of this type of failure was considerably reduced when compared to results of testing on the brickwork pattern. Rushing and Tingle (2007) reported the first rail failure (upper underlap) after only 384 passes, whereas the first in this test was documented after 1,700 passes. The authors also reported at least seven panels with either upper underlap or lower overlap rail failure at the end of the test (1,792 passes). For the 2-1 lay pattern test, rail failures were observed at nearly all sections with two continuous joints along the centerline (Figure 1). The increased length in support between joints along the centerline with the modified 2-1 lay pattern was likely the key contributor in better end connector performance. The inclusion of the fillet in the corners of the locking bar channel might have also contributed to this behavior by decreasing stress concentrations in those areas, thus improving the fatigue life by inhibiting crack incubation from occurring at low cycles.

Top skin tearing occurs because of shear forces subjected at the corner of the top skin of panels with joints along the centerline. A skin tear began as

the corner curled upward or when a minor crack developed at the weld but always propagated along the top flange of the female hinge. When the test tire was located along the joint, the top flange of the female hinge at the south edge pulled at the connecting male hinge for support. As cracking started to develop at (or near) the panel south corner, the top flange required support further away from the joint, causing cracking to propagate along its length with increasing load repetitions. Rushing and Tingle (2007) reported at least seven panels to have failed by top skin tearing along the female hinge when they tested the brickwork pattern, a number that was significantly reduced in this test.

Core crushing occurred in three panels due to buckling of the vertical members in the mat core. Rushing and Tingle (2007) reported at least two panels to have failed by core damage in their testing. The initial sign of core crushing was dishing observed on the surface. As the panel structure continued to collapse with increasing load repetitions, the dished area became larger. Top and bottom skin cracking parallel to the vertical stiffeners were characteristics of this failure mechanism. Cracking developed because the skins could no longer accommodate the bending action of the load without the support from the stiffeners.

As expected, the modified 2-1 lay pattern provided increased performance when compared to the 2-1 lay pattern. Moreover, it exceeded the load-carrying capabilities of the brickwork pattern by more than 1,000 passes. When compared to results reported by Garcia et al. (in preparation) for the filleted AM2 design, the passes-to-failure were increased by nearly 600 F-15E passes. The data are encouraging for improvements to the AM2 mat system, especially at the end connector design.

5.2 Permanent deformation

5.2.1 Centerline profile

The centerline profiles for the post-traffic subgrade and the surface of the mat at various traffic intervals were analyzed to determine whether the roughness criteria were exceeded. The maximum values for the subgrade and mat surface at the end of the test were both below the 1.25-in.-deep maximum value established for roughness for F-15E aircraft traffic. Therefore, the system performed adequately to prevent excessive roughness from occurring along the centerline. This behavior was expected, since the AM2 mat system has generally functioned well in preventing excessive

roughness along the centerline profile when placed on a CBR of 6, as reported by Rushing and Tingle (2007), Rushing and Torres (2007), Rushing et al. (2014), and Garcia et al. (in preparation).

5.2.2 Cross sections

The permanent deformation on the subgrade, the loaded mat surface, and the unloaded mat surface were analyzed to determine whether the deformation criteria were exceeded. After 2,850 passes, these values were 1.74 in., 1.34 in., and 0.66 in., respectively. Although the deformation on the loaded mat surface exceeded the failure criterion of 1.25 in., it occurred after mat breakage failure was achieved. The subgrade deformation also exceeded the criterion. However, since the subgrade surface deformation was determined after the mat panels were removed, the number of passes at which the 1.25-in. rut was developed could not be determined. Therefore, failure was assumed at pass 2,638 due to mat breakage, even if the subgrade surface exceeded the limit beforehand.

Rushing and Tingle (2007) reported an unloaded surface deformation of 0.44 in. and a subgrade surface deformation of almost 1.25 in. at the end of the test (1,792 passes) for the brickwork pattern. In this test, the unloaded surface deformation at approximately the same pass level (plot for pass level 1,728 in Figure 35) was 0.29 in. The loaded surface deformation (i.e., approximate subgrade deformation) was 0.87 in., according to Figure 36. Both of these values are well below those measured by Rushing and Tingle (2007), further evidence of improved performance with increased support between joints in the wheel path. The system, therefore, worked well in reducing deformation on the surface at low cycles.

5.3 Elastic deflection

Historically, elastic deflection measurements were used to monitor performance of mat systems but were not used for mat system fatigue failure criteria. Average elastic deflection of the mat and subgrade increased throughout testing to 1.5 in. at the end of the test. Assuming that the elastic deflection of the subgrade remained nearly constant throughout traffic, the increase in the total elastic deflection of the mat and subgrade indicates that the air gap beneath the mat increased as deformation occurred in the subgrade surface. As expected, the average elastic deflection at the joints was higher throughout testing than at the offset locations (3-ft offset from the joint). At the end of the test, elastic

deflection at the joint and offset locations were approximately 1.27 in. and 1.25 in., respectively. Rushing and Tingle (2007) reported similar values of elastic deflection at the joint and center panel locations for the brickwork pattern, which were up to 1.3 in. and 1.1 in., respectively.

6 Conclusions and Recommendations

6.1 Conclusions

The purpose of this effort was to conduct a full-scale test of the AM2 mat system under simulated F-15E traffic when installed over a subgrade with a CBR of 6 in a modified 2-1 lay pattern. Recent investigations showed that the AM2 2-1 lay pattern approved by NAVAIR for use on all aircraft operating surfaces reduced the performance of the system when compared against baseline standards for an AM2 surface placed on a CBR of 6, which requires a minimum of 1,500 F-15E and C-17 passes. This was largely attributed to the sections that consisted of two continuous end joints, where premature, consecutive rail failures occurred due to reduced support on each 2-ft end. Therefore, a modified 2-1 lay pattern was tested to determine whether improved load-carrying capacity could be exhibited by the AM2 mat system when the rows were staggered, effectively offsetting the joints by 3 ft. AM2 panels produced with filleted corners in the locking bar channel were installed along the wheel path to provide additional insight on the performance of the recently corrected end connector design at a critical stress location. Permanent deformation and mat breakage were monitored. The results of the tests were used to determine whether an increase in the number of passes-to-failure could be achieved with the modified installation pattern.

The following conclusions were derived from accelerated traffic testing of the AM2 airfield matting system conducted in October 2014:

- The AM2 mat system when installed in the modified 2-1 lay pattern on a CBR of 6 was able to withstand 2,638 passes of simulated F-15E traffic before failure by mat breakage. This represents a 75 percent increase in the number of passes-to-failure from the baseline brickwork pattern test on a subgrade with a CBR of 6. It should be noted that some variation in performance between replicate full-scale tests would be expected. However, the magnitude of the increase in sustained aircraft passes before failure demonstrates a significant performance increase.
- Improved performance was noted at the end connector due to an increase in the length of support between the joints along the wheel path when compared to the 2-1 lay pattern. Additionally, the filleted

corners in the locking bar channel were assumed to contribute considerably to the limited number of rail failures.

6.2 Recommendations

Based on the results of the evaluation discussed in this report, it is recommended that alternatives to the current design of the AM2 mat system be investigated. This includes the addition of different panel sizes (e.g., 3-ft-long panel) and alternative patterns that increase support conditions between longitudinal joints.

References

ASTM International. 2007. *Standard test method for CBR of laboratory compacted soils*. Designation: D 1883. West Conshohocken, PA: ASTM International.

_____.2007. *Standard test method for density and unit weight of soil in place by the sand cone method*. Designation: D 1556. West Conshohocken, PA: ASTM International.

_____. 2007. *Standard test methods for liquid limit, plastic limit, and plasticity index of soils*. Designation: D 4318. West Conshohocken, PA: ASTM International.

_____. 2007. *Standard test method for particle size analysis of soils*. Designation: D 422. West Conshohocken, PA: ASTM International.

_____. 2009. *Standard test method for use of the dynamic cone penetrometer in shallow pavement applications*. Designation: D 6951. West Conshohocken, PA: ASTM International.

_____. 2010. *Standard test method for density of soil in place by the drive cylinder*. Designation: D 2937. West Conshohocken, PA: ASTM International.

_____. 2010. *Standard test method for in-place density and water content of soil and soil-aggregate by nuclear methods (shallow depth)*. Designation: D 6938. West Conshohocken, PA: ASTM International.

_____. 2010. *Standard test methods for laboratory determination of water (moisture) content of soil and rock by mass*. Designation: D 2216. West Conshohocken, PA: ASTM International.

_____. 2011. *Standard practice for classification of soils for engineering purposes (USCS)*. Designation: D 2487. West Conshohocken, PA: ASTM International.

_____. 2012. *Standard test method for laboratory compaction characteristics of soil using modified effort*. Designation: D 1557. West Conshohocken, PA: ASTM International.

Garcia, L., T. W. Rushing, and Q. S. Mason. 2012. *Evaluation of Webcore Prototype AMX Mat System*. ERDC/GSL TR-12-14. Vicksburg, MS: U.S. Army Engineer Research and Development Center.

Garcia, L. T., and T. W. Rushing. 2013. *AM2 sand subgrade sensitivity test*. ERDC/GSL TR-13-10. Vicksburg, MS: U.S. Army Engineer Research and Development Center.

Garcia, L., T. W. Rushing, and Q. S. Mason. 2014a. *AM2 25 CBR subgrade sensitivity test*. ERDC TR-14-7. Vicksburg, MS: U.S. Army Engineer Research and Development Center.

Garcia. L. , T. W. Rushing, B. A. Williams, and C. A. Rutland.2014b. *AM2 100 CBR subgrade sensitivity test*. ERDC TR-14-37. Vicksburg, MS: U.S. Army Engineer Research and Development Center.

Garcia, L., T. W. Rushing, Q.S. Mason, J. S. Tingle, and C.A. Rutland. (in preparation). *AM2 mat end connector modeling and performance validation*. ERDC/GSL TR-15-X. Vicksburg, MS: U.S. Army Engineer Research and Development Center.

Naval Air Warfare Center. 2006. *Expeditionary airfield AM2 mat certification requirements*. NAWCADLKE-MISC-48J200-0011. Lakehurst, NJ: Naval Air Warfare Center, Aircraft Division.

Rushing, T. W., and J. S. Tingle. 2007. *AM2 and M19 Airfield mat evaluation for the Rapid Parking Ramp Expansion Program*. ERDC/GSL TR-07-5. Vicksburg, MS: U.S. Army Engineer Research and Development Center.

Rushing, T. W., and N. Torres. 2007. *Prototype mat system evaluation*. ERDC/GSL TR-07-29. Vicksburg, MS: U.S. Army Engineer Research and Development Center.

Rushing, T. W., and Q. S. Mason. 2008. *AM2 15 CBR subgrade sensitivity test for the rapid parking ramp expansion program*. ERDC/GSL TR-08-25. Vicksburg, MS: U.S. Army Engineer Research and Development Center.

Rushing, T. W., N. Torres, and Q. Mason. 2008. *AM2 10 CBR subgrade sensitivity test for the Rapid Parking Ramp Expansion Program*. ERDC/GSL TR-08-13. Vicksburg, MS: U.S. Army Engineer Research and Development Center.

Rushing, T. W., L. Garcia, and Q. S. Mason. 2011. *Large-scale 6-CBR prototype mat system evaluation for the AMX program*. ERDC/GSL TR-11-37. Vicksburg, MS: U.S. Army Engineer Research and Development Center.

Rushing, T. W., L. Garcia, and Q. S. Mason. 2012. *Evaluation of Faun aluminum mat systems*. ERDC/GSL TR-12-32. Vicksburg, MS: U.S. Army Engineer Research and Development Center.

Rushing, T.W., L. Garcia, J.S. Tingle, P.G. Allison, and C.A. Rutland. 2014. *AM2 3-4 alternate lay pattern evaluation*. ERDC/GSL TR-14-38. Vicksburg, MS: U.S. Army Engineer Research and Development Center.

U.S. Army Engineer Research and Development Center (ERDC). 1995. *Standard test method for California bearing ratio of soils in place*. Designation: CRD-C654-95. Vicksburg, MS: U.S. Army Engineer Research and Development Center.

REPORT DOCUMENTATION PAGE

Form Approved
OMB No. 0704-0188

1. REPORT DATE *(DD-MM-YYYY)*	2. REPORT TYPE	3. DATES COVERED *(From - To)*
August 2015	Final report	

4. TITLE AND SUBTITLE

AM2 Modified 2-1 Lay Pattern Evaluation under F-15E Traffic

5a. CONTRACT NUMBER

5b. GRANT NUMBER

5c. PROGRAM ELEMENT NUMBER

6. AUTHOR(S)

Lyan Garcia, Julie Heiser, Timothy W. Rushing, Chase T. Bradley, Jeb S. Tingle, and Craig A. Rutland

5d. PROJECT NUMBER

5e. TASK NUMBER

5f. WORK UNIT NUMBER

7. PERFORMING ORGANIZATION NAME(S) AND ADDRESS(ES)

U.S. Army Engineer Research and Development Center
Geotechnical and Structures Laboratory
3909 Halls Ferry Road
Vicksburg, MS 39180-6199

8. PERFORMING ORGANIZATION REPORT NUMBER

ERDC/GSL TR-15-32

9. SPONSORING / MONITORING AGENCY NAME(S) AND ADDRESS(ES)

Headquarters, Air Force Civil Engineer Center
Tyndall Air Force Base, FL 32403-5319

10. SPONSOR/MONITOR'S ACRONYM(S)

11. SPONSOR/MONITOR'S REPORT NUMBER(S)

12. DISTRIBUTION / AVAILABILITY STATEMENT

Approved for public release; distribution is unlimited.

13. SUPPLEMENTARY NOTES

14. ABSTRACT

The U.S. Army Engineer Research and Development Center executed a program for the Air Force Civil Engineer Center and the Naval Air Systems Command (NAVAIR) that involved a series of full-scale tests of the AM2 airfield mat system in an effort to validate a model which predicts the performance of AM2 under different operational conditions. A key component of the test program was evaluating the AM2 installation patterns approved by NAVAIR, which included the 2-1 lay pattern that is used on runways and high-speed taxiways. Initial analyses of the results showed that the performance of the AM2 mat system installed in the 2-1 lay pattern decreased when compared to the standard brickwork pattern, largely because of sections resulting with two longitudinal joints. An alternative pattern was sought to improve the load-carrying capabilities of the system, and the results are provided in this report. The discussions herein summarize traffic tests that were conducted on what was called the "modified" 2-1 lay pattern, which amended the 2-1 lay pattern to eliminate the key contributor that reduced system performance (i.e., two continuous joints). The results showed a significant increase in passes-to-failure in comparison to the 2-1 lay pattern and the brickwork pattern.

15. SUBJECT TERMS

AM2
Landing mat
Aluminum mat
Airfield mat
Airfield damage repair
Expeditionary airfield mat

16. SECURITY CLASSIFICATION OF:			17. LIMITATION OF ABSTRACT	18. NUMBER OF PAGES	19a. NAME OF RESPONSIBLE PERSON
a. REPORT	b. ABSTRACT	c. THIS PAGE			19b. TELEPHONE NUMBER *(include area code)*
UNCLASSIFIED	UNCLASSIFIED	UNCLASSIFIED		54	